

## Chapter 4

### Optimal Path Simulation

This chapter includes the outline of the optimal path simulation setup, detailed description of simulation test track, and parameters of each case.

#### 4.1 Simulation Test Tracks

Initially, the geometry of an actual test track was to be used as the constrained road for the optimal path simulation. It was quickly realized that the simulation time necessary to complete one run would be in the magnitude of days, using a 266 MHz Pentium II processor with 64 MB of RAM. The size of the track was then reduced to small sections, without sacrificing the content of the simulation results.

The test track is divided into modular sections such that the sections can be added or subtracted easily. Each modular section consists of a starting position, ending position, and a slope, as shown in Figure 4.1. A linear equation is used to describe the track to simplify the simulation by making it easier to define the path constraint as shown in Eqs. (3.11) – (3.13).

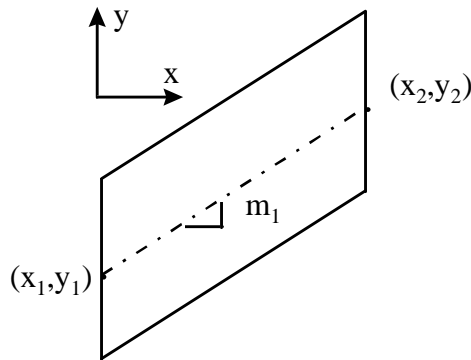


**Figure 4.1 A Modular Test Track Section**

Two different test tracks are used in this simulation, one containing two sections and another containing three sections, as shown in Figure 4.2, to demonstrate the application and effectiveness of the modular test track idea.

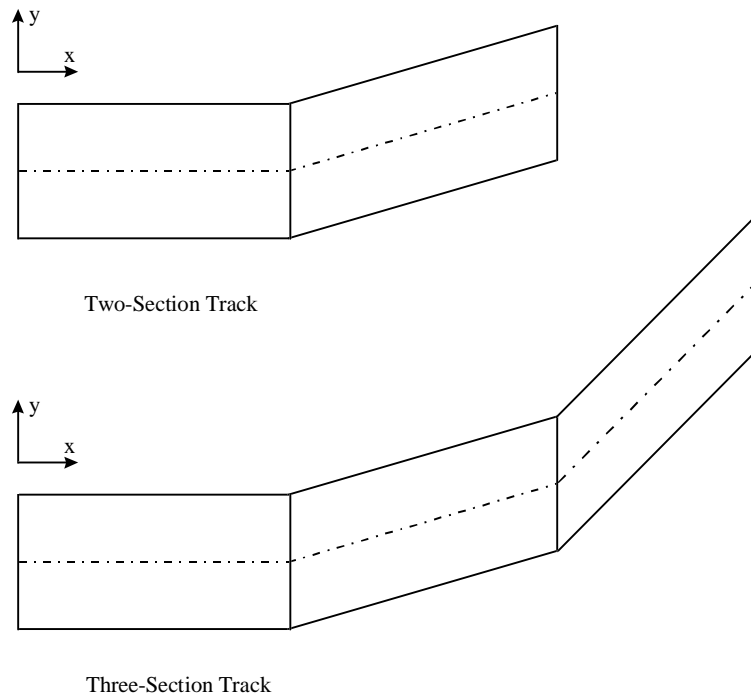


**Figure 4.2 Simulation Test Tracks**

The width of the track is defined as 1 meter from the centerline to each side of the track, therefore the total width is equal to 2 meters. This may seem narrow, however, this is a restriction on the center of gravity of the vehicle, not the entire body of the vehicle.

## 4.2 Optimal Path Simulation

The simulation requires an initial set of system inputs (i.e., steering angle and longitudinal force) along with an initial execution time for each of the modular section. The execution time for each section will vary depending on the steering angle and longitudinal force. When all of the sections are added, the initial set of system inputs is then consisted of a series of steering angles, longitudinal forces, and time. The entire path is executed once before the cost function is evaluated. Care must be taken when selecting the initial values of the system inputs because they directly influence the computation time and convergence.

The steering angle input for the simulation consists of two types, a step function and a sinusoidal function. Two types are used to demonstrate the effectiveness of the optimization algorithm.

The longitudinal force input is kept constant for each section of the road. The idea is that each section is selected to be small enough, therefore keeping the longitudinal force constant and reducing the likelihood of generating erroneous results.

The initial conditions of the dynamic variables must also be given, they define the initial state of the vehicle. The initial orientation of the vehicle will be given at the beginning of the discussion of each test case.

### 4.3 Simulation Cases

The simulation of this research can be divided into two major categories, corresponding to the two objectives of the simulation, namely the minimum time objective and maximum tire force objective. Within each one of these objectives there are sub-categories consisted of different road geometries, steering inputs, and initial velocity. Table 4.1 shows the cases considered for the simulation.

**Table 4.1 Simulation Cases**

Case No.	Track	Objective	Steering Angle Input	Initial Velocity
1	Two-section	Minimize time	Step	10
2	Two-section	Minimize time	Step	20
3	Two-section	Minimize time	Sine	10
4	Three-section	Minimize time	Step	10
5	Two-section	Max tire force	Step	10
6	Two-section	Max tire force	Step	20
7	Two-section	Max tire force	Sine	10
8	Three-section	Max tire force	Step	10

## 4.4 Minimum Time Simulation

The objective of this simulation is to determine an optimal path that would minimize the travel time of the vehicle. Four cases are simulated to demonstrate the effectiveness of the optimization algorithm and to show that it can be used to determine an optimal path. The total time for the vehicle to get to the desired position is evaluated for each case. They are believed to be minimized due to the fact that the scalar value of the cost function is minimized.

### 4.4.1 Two-Section Test Track

Figure 4.3 shows the two-section test track used for this particular simulation.

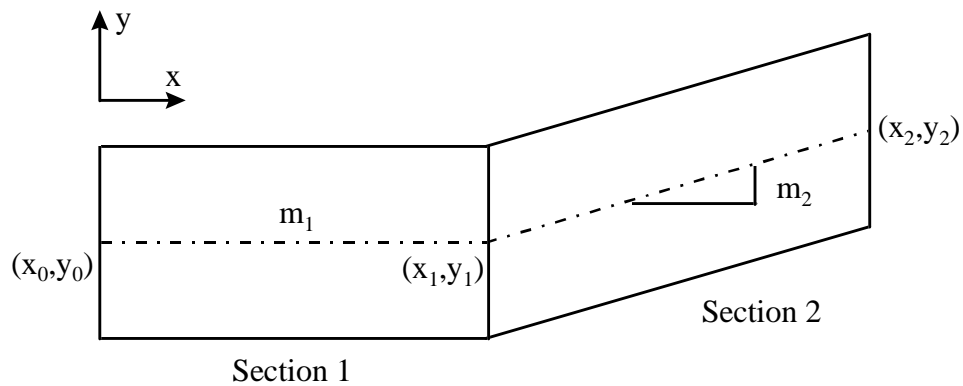


**Figure 4.3 Two-Section Test Track**

Table 4.3 lists the coordinates and the slopes of the track.

**Table 4.2 Two-Section Test Track Specifications**

Track Section	X end position (m)	Y end position (m)	Slope
1	5.194	0	0
2	10.668	0.435	0.794

#### 4.4.1.1 Step Steering Angle Input

The first case of steering angle input is a step steering type. For each section of the track, the optimization routine is allowed to adjust the amplitude of the step steering angle to obtain the optimal solution, satisfying the minimum time objective. The optimization algorithm is also allowed to adjust the time for each section, since the execution time may vary from one section to another. Table 4.3 lists the values of the initial system inputs for each of the track sections.

**Table 4.3 Values of Initial System Inputs for Step Input/Two-Section Track**

Track Section	Variable	Value
1	$\delta$	0 deg
	$P_f$	2000 N
	t	0.5 sec
2	$\delta$	45 deg
	$P_f$	2000 N
	t	0.5 sec.

where

$\delta$  = steering angle

$P_f$  = longitudinal force

t = time

##### 4.4.1.1.1 Case No. 1: Minimum Time, $V_\eta = 10$ m/s, Step Input

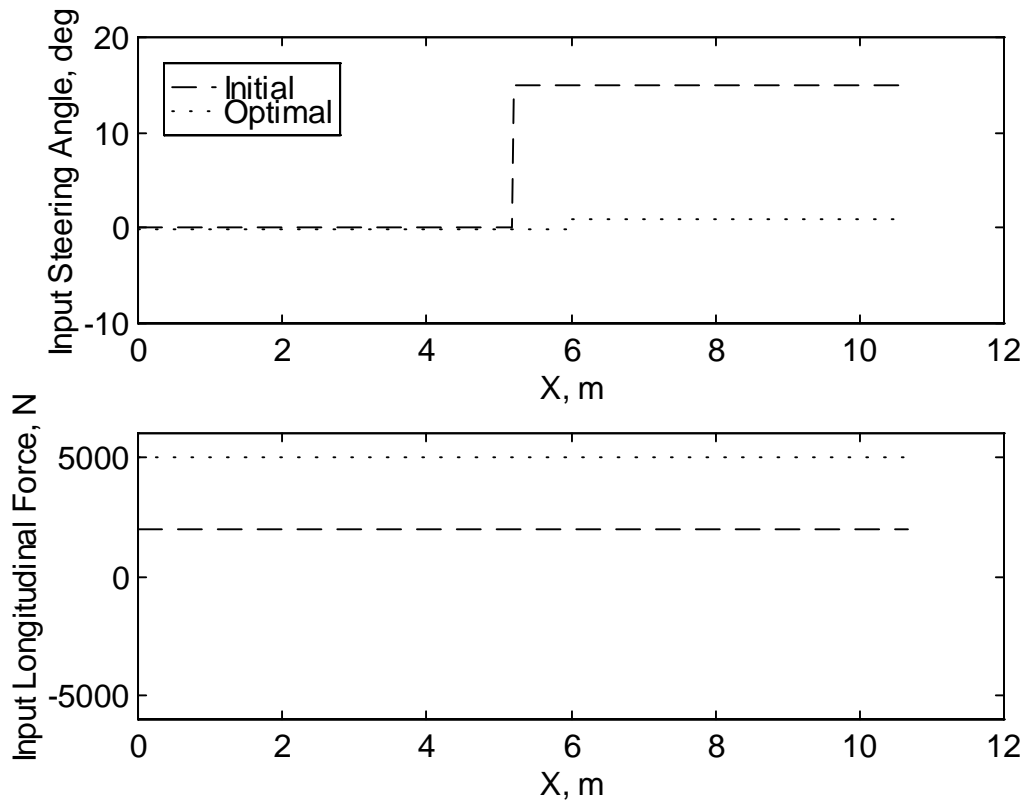
For Case No. 1, the system inputs are a series of step steering angles, and a constant longitudinal force as shown in Table 4.3. These values were selected such that the initial response of the vehicle is moderate and the vehicle stays within the boundaries of the track.

Table 4.4 lists the initial conditions of the dynamic variables.

**Table 4.4 Case No. 1: Initial Values of the Step, Two-Section Track Simulation**

Variable	Value
$X_1$	0
$X_2$	0
$X_3$	10
$X_4$	0
$X_5$	0
$X_6$	0
$X_7$	0
$X_8$	0
$X_9$	0
$X_{10}$	0
$X_{11}$	0

Figure 4.4 shows the optimized steering angle and longitudinal force, as indicated the dotted line plotted against the initial condition indicated by the dashed line.



**Figure 4.4 Case No. 1 Optimal System Input**

As anticipated, the steering angle is very close to zero since the quickest path the vehicle can take is a straight line while complying to the path constraint. Also as anticipated, the longitudinal force is at full throttle, 5000 N, since the quickest way to get to the desired destination is full acceleration. These two optimal system inputs seem to comply with intuition.

Table 4.5 lists the values of the optimal system input variables and time.

**Table 4.5 Values of Optimal System Inputs for Step Input/Two-Section Track**

Track Section	Variable	Value
1	$\delta$	-0.129 deg
	$P_f$	5000 N
	t	0.544 sec
2	$\delta$	1.014 deg
	$P_f$	5000 N
	t	0.361 sec.

where

$\delta$  = steering angle

$P_f$  = longitudinal force

t = time

The execution time of the first track section actually increased by 8.8% to 0.544 sec. The second section of the track, however, has a significant reduction, 27.8% to 0.361 sec. Therefore it can be seen that the minimum time objective has been met by the optimization algorithm with a total reduction in execution time of 9.5% to 0.905 sec.

Figure 4.5 shows the optimal path of the vehicle, indicated by the dotted line, plotted against the initial condition indicated by the dashed line.



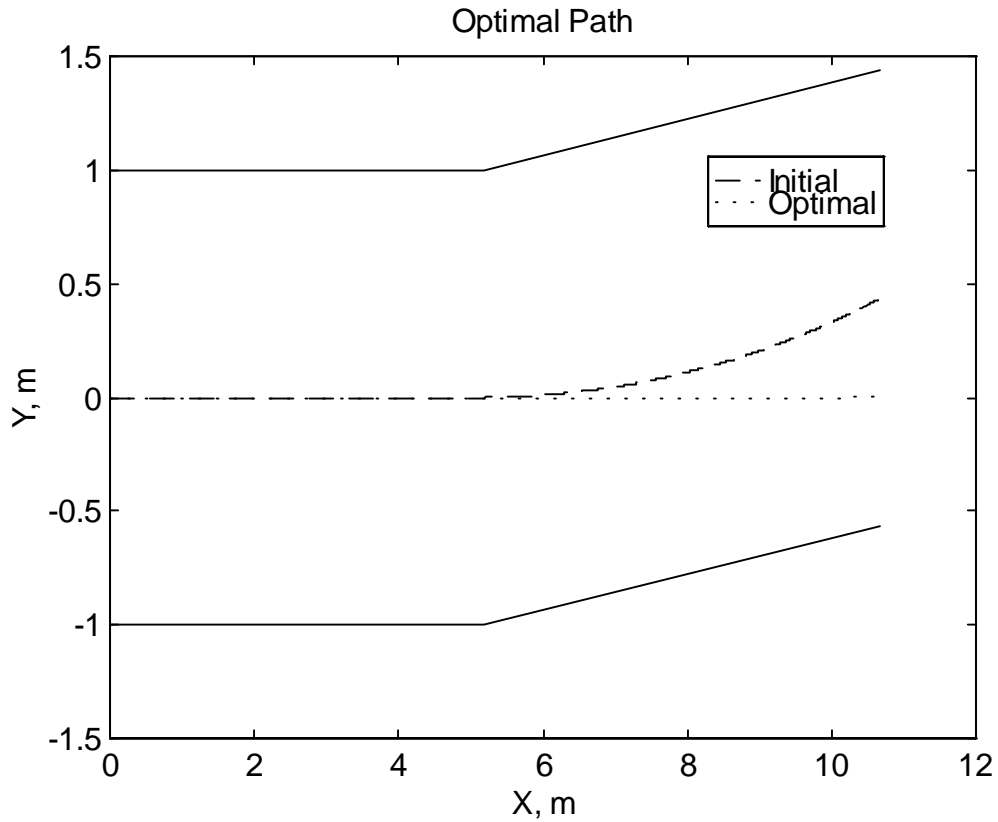


**Figure 4.5 Case No. 1 Optimal Vehicle Path**

As can be seen, the optimal path is very close to a straight line. This is anticipated since the quickest path between two points is a straight line.

Figure 4.6 shows the lateral position, the lateral velocity, and the lateral acceleration of the vehicle at the optimal condition.

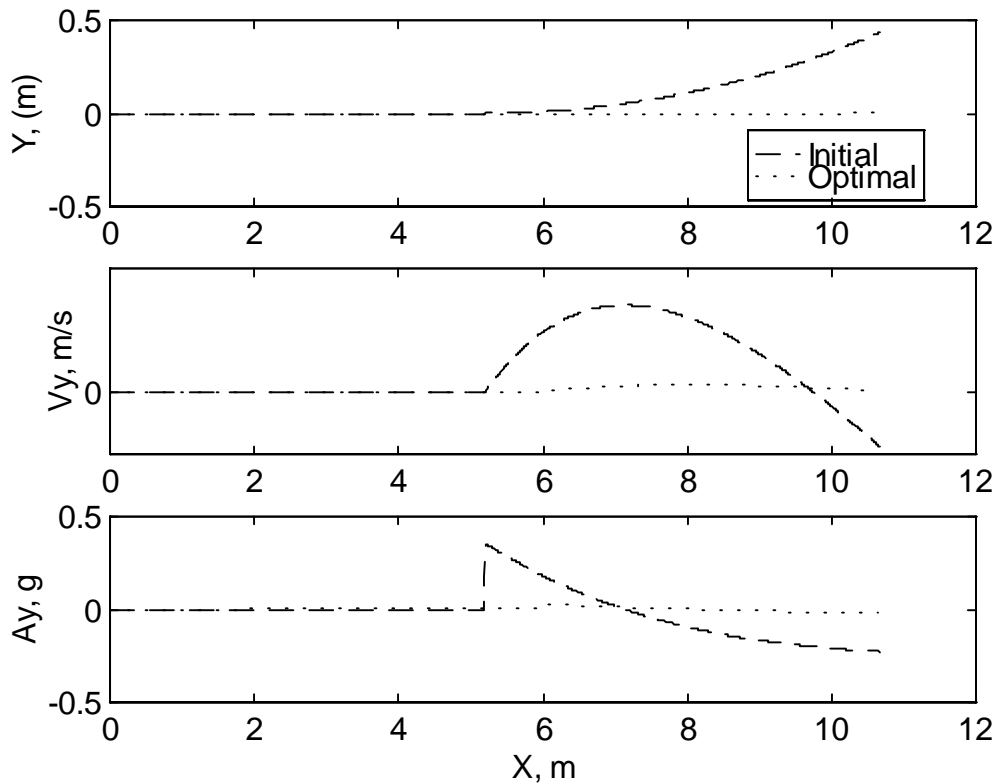


**Figure 4.6 Case No. 1: Lateral Position, Lateral Velocity, & Lateral Acceleration**

These variables are shown to be very close to zero. Small positive step jumps can be seen on the optimal lateral velocity and acceleration. These jumps can be explained by the small step steering angle to the positive direction at about the same point along the longitudinal direction. The lateral behavior of the vehicle is almost nonexistent when the vehicle is traveling in a straight.

Figure 4.7 shows the longitudinal velocity, the yaw angle, and the yaw velocity of the vehicle at the optimal condition.

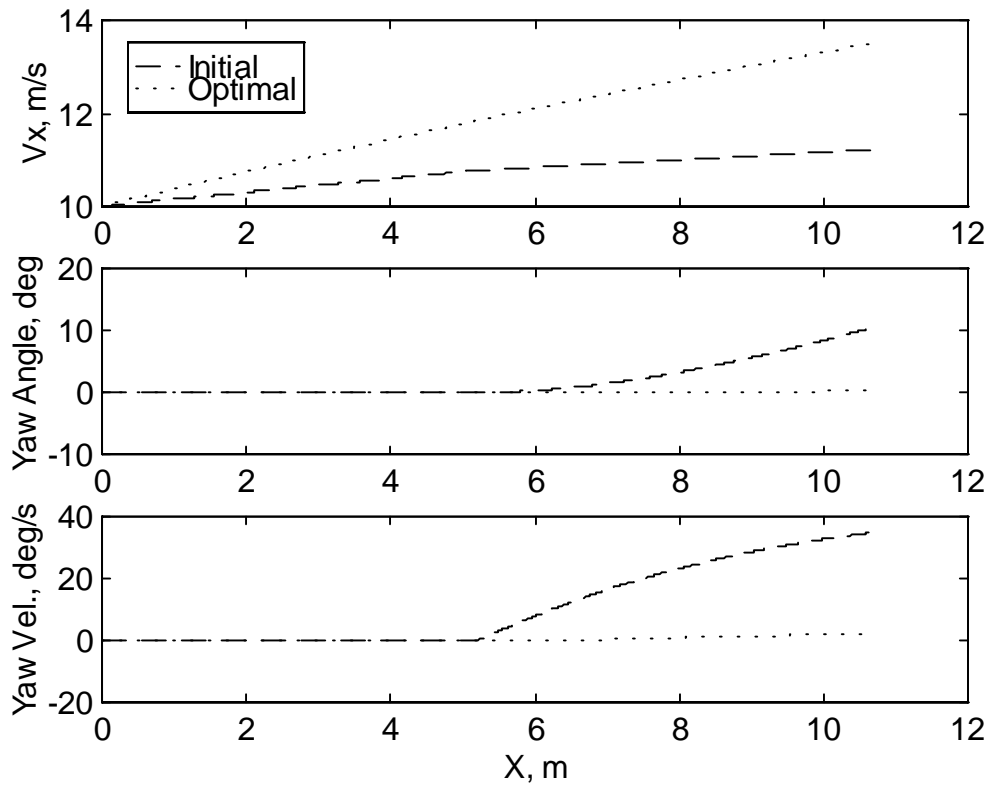


**Figure 4.7 Case No. 1: Longitudinal Velocity, Yaw Angle, & Yaw Velocity**

The longitudinal velocity shows a steady increase since the longitudinal force applied to the vehicle is constant at full throttle for the entire path. The optimal yaw angle and velocity are almost zero for the entire path, corresponding to almost nonexistent lateral motion of the vehicle.

Figure 4.8 shows the lateral force, the slip angle, and the speed constraint, indicated by the dotted line, plotted against the initial condition indicated by the dashed line.

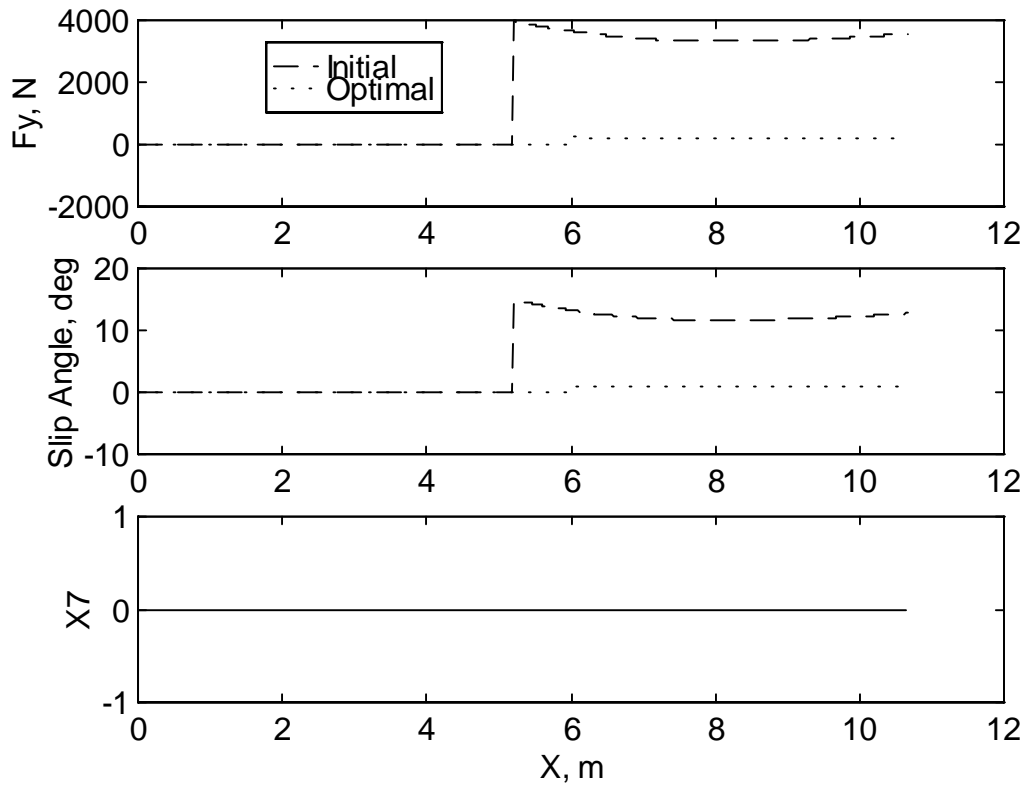


**Figure 4.8 Case No. 1: Lateral Force, Slip Angle, & Vehicle Speed Constraint**

The optimal lateral force and slip angle show zero amplitude for the reason mentioned above. The speed constraint variable is zero for the entire path because the maximum speed of 120 mph (27.0 m/s) is not exceeded.

Figure 4.9 shows the path constraint variable, the steering angle constraint variable, and the longitudinal force constraint variable.

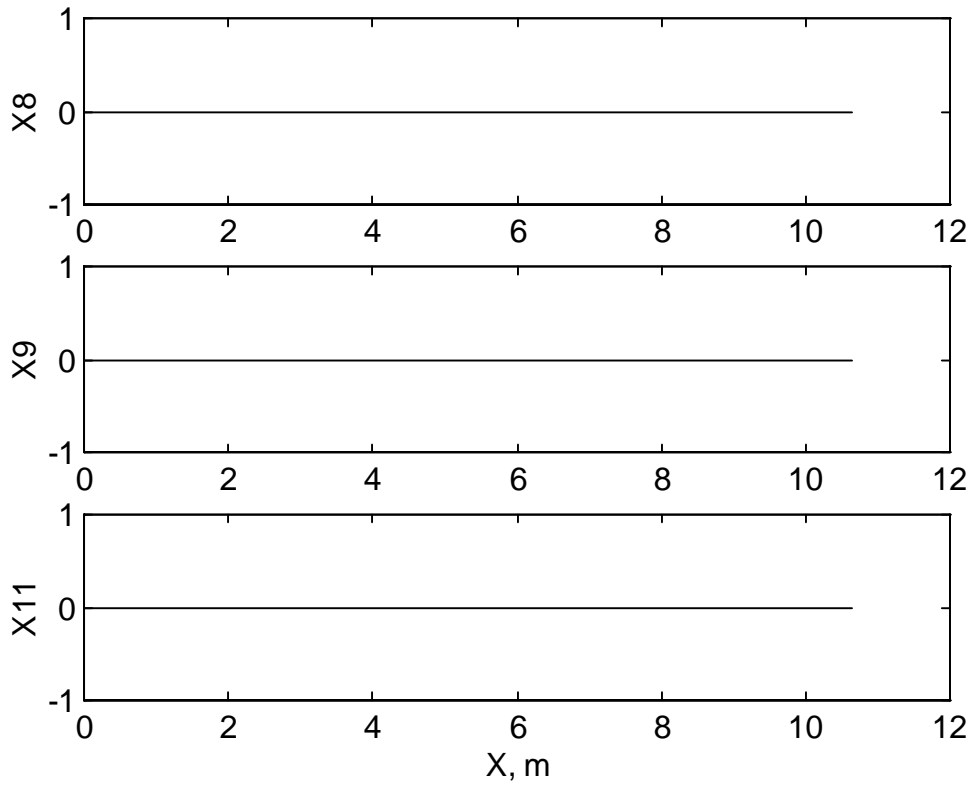


**Figure 4.9 Case No. 1: Path Constraint ( $x_8$ ), Steering Angle Constraint ( $x_9$ ), & Longitudinal Force Constraint ( $x_{11}$ )**

None of these variables exceeded the constraint condition defined in the penalty functions, Eqs (3.8), (3.10), and (3.13) therefore their values are zero throughout the path.

#### 4.4.1.1.2 Case No. 2: Minimum Time, $V_{\eta} = 20$ m/s, Step Input

For Case No. 2, Table 4.6 lists the initial conditions of the dynamic variables.

**Table 4.6 Case No. 2: Initial Values of Step/Two-Section Track Simulation**

Variable	Value
$X_1$	0
$X_2$	0
$X_3$	20
$X_4$	0
$X_5$	0
$X_6$	0
$X_7$	0
$X_8$	0
$X_9$	0
$X_{10}$	0
$X_{11}$	0

The system inputs are a series of step steering angles, and a constant longitudinal force as shown in Figure 4.10, the optimized steering angle and longitudinal force are indicated by the dotted line, while the initial condition are indicated by the dashed line.

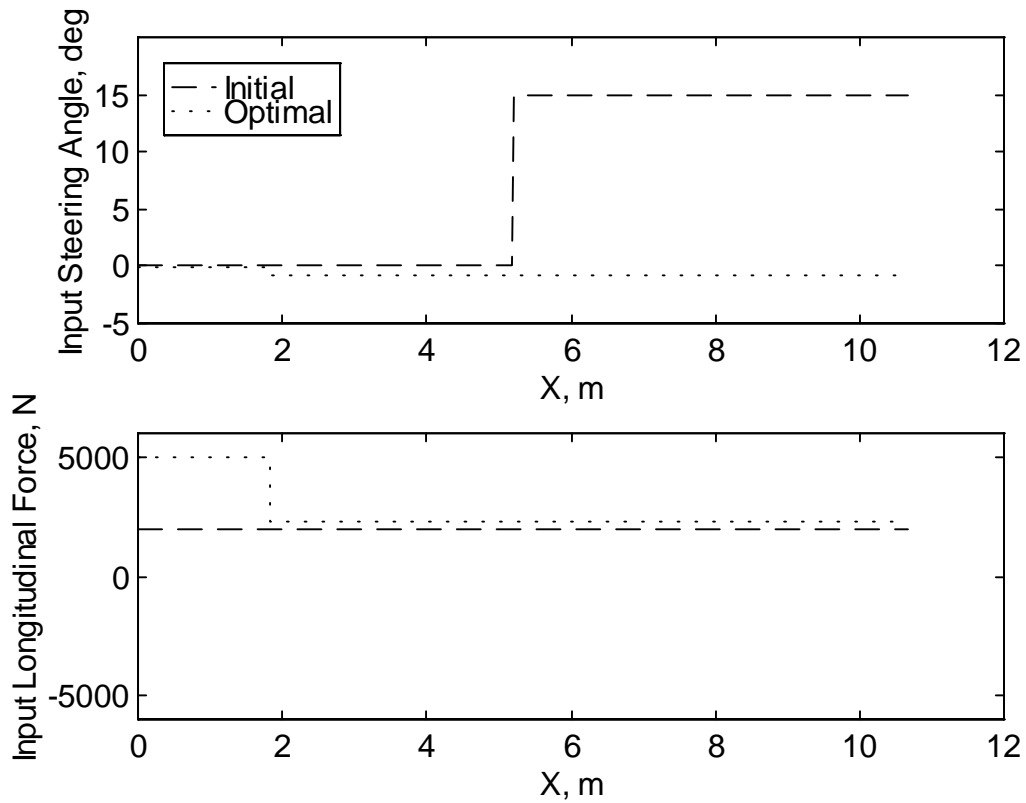


**Figure 4.10 Case No. 2 Optimal System Input**

As anticipated, the steering angle is very close to zero since the quickest path the vehicle can take is a straight line while complying with the path constraint. However, the longitudinal force could still be optimized more. For the first section, the optimization routine is able to increase the longitudinal force to 5000 N. For the second section, the longitudinal force optimized on a value of 2313.8 N due to limitation of the computation time. This value could definitely be improved with a faster processor computer.

Table 4.7 lists the values of the optimal system input variables and time.

**Table 4.7 Case No. 2 Optimal System Inputs for Step Input/Two-Section Track**

Track Section	Variable	Value
1	$\delta$	-0.179 deg
	$P_f$	5000 N
	t	0.090 sec
2	$\delta$	0.854 deg
	$P_f$	2313.8 N
	t	0.427 sec.

where

$\delta$  = steering angle

$P_f$  = longitudinal force

t = time

The execution time of the first track section decreased by 82% to 0.090 sec. The second section of the track has a reduction, 7.3% to 0.427 sec. Therefore it can be seen that the minimum time objective has been met by the optimization algorithm with a total reduction in execution time by 48.3% to 0.517 sec with an initial velocity of 20 m/s.

Figure 4.11 shows the optimal path of the vehicle, indicated by the dotted line, plotted against the initial condition indicated by the dashed line.



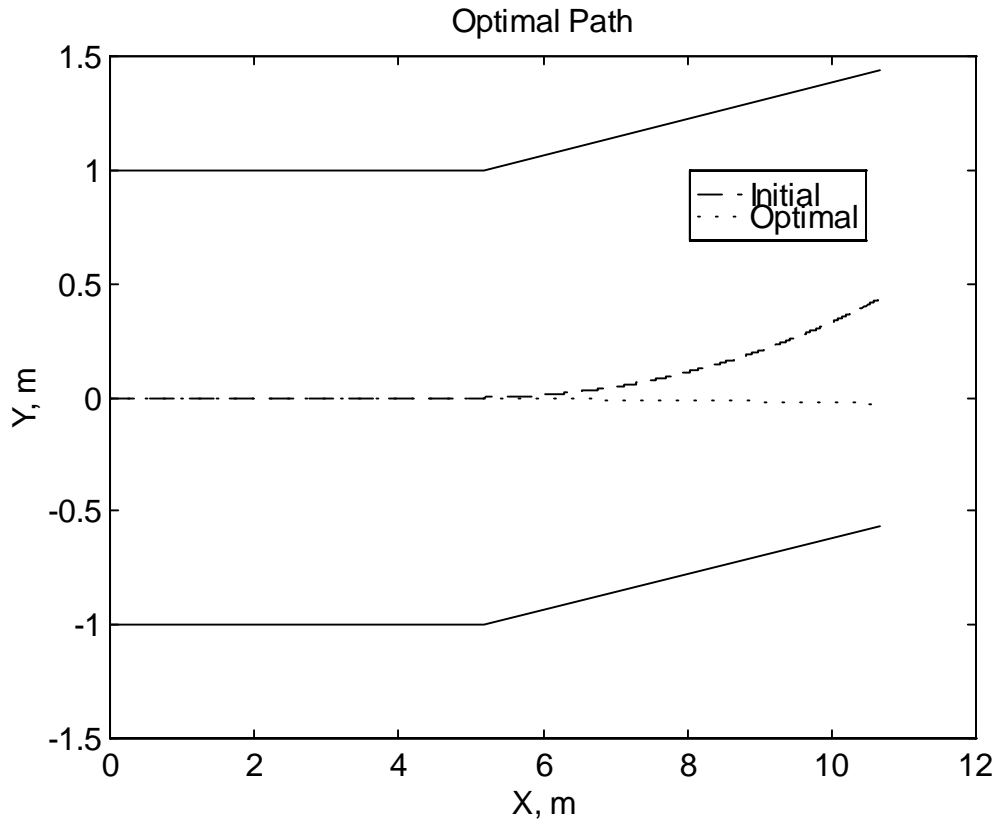


**Figure 4.11 Case No. 2 Optimal Vehicle Path**

As can be seen, the path is very close to a straight line. This is anticipated since the quickest path between two points is a straight line.

Figure 4.12 shows the lateral position, the lateral velocity, and the lateral acceleration of the vehicle at the optimal condition.

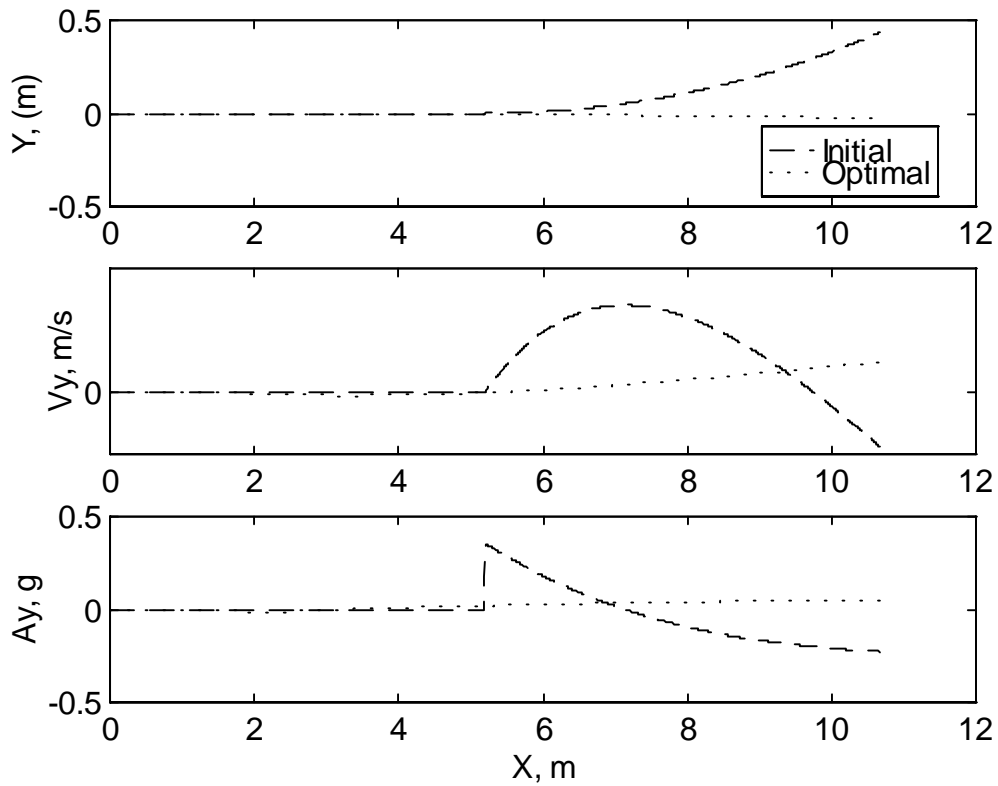


**Figure 4.12 Case No. 2: Lateral Position, Lateral Velocity, & Lateral Acceleration**

The lateral position demonstrates a small negative deviation towards the end of the path corresponding to small negative steering angle. The optimal lateral velocity and acceleration show positive deviations towards the end of the path. This could be due to minute increase in the steering angle near the end of the path.

Figure 4.13 shows the longitudinal velocity, the yaw angle, and the yaw velocity of the vehicle at the optimal condition.

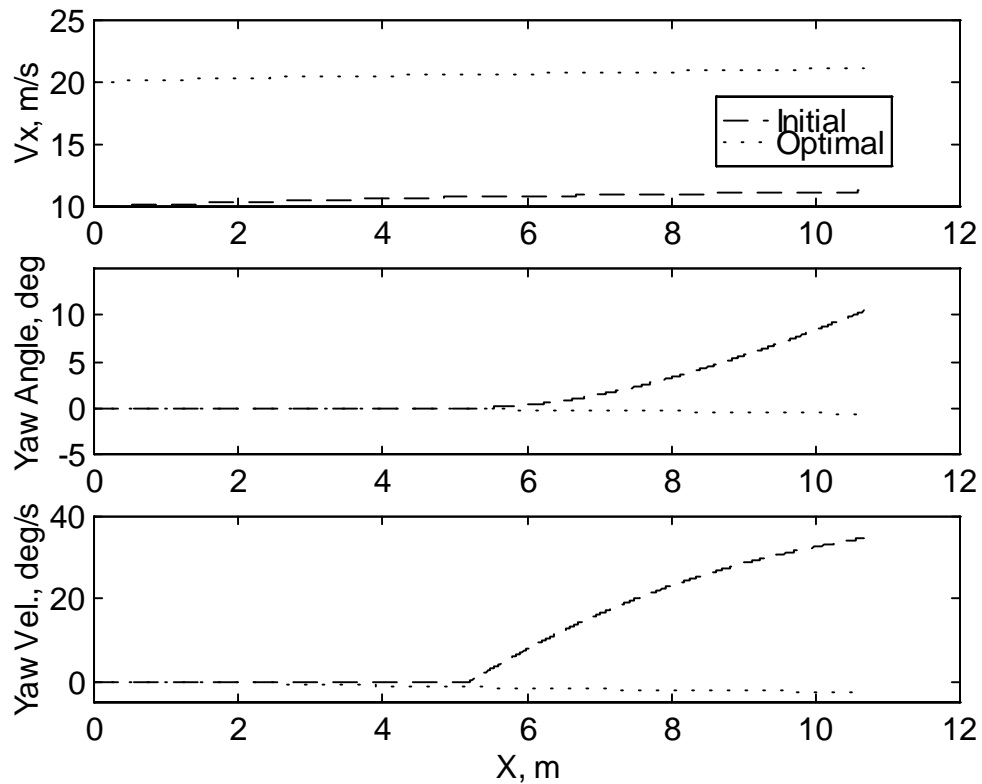


**Figure 4.13 Case No. 2: Longitudinal Velocity, Yaw Angle, & Yaw Velocity**

The longitudinal velocity shows a slow increase since the longitudinal force applied to the vehicle is no longer at full throttle for the entire path. It is initial high, 5000 N, but then levels off to approximately 2500 N. The optimal yaw angle and velocity shows the same trend as the vehicle path, deviating to the negative direction towards the end of the path.

Figure 4.14 shows the optimal lateral force, the slip angle, and the speed constraint condition.

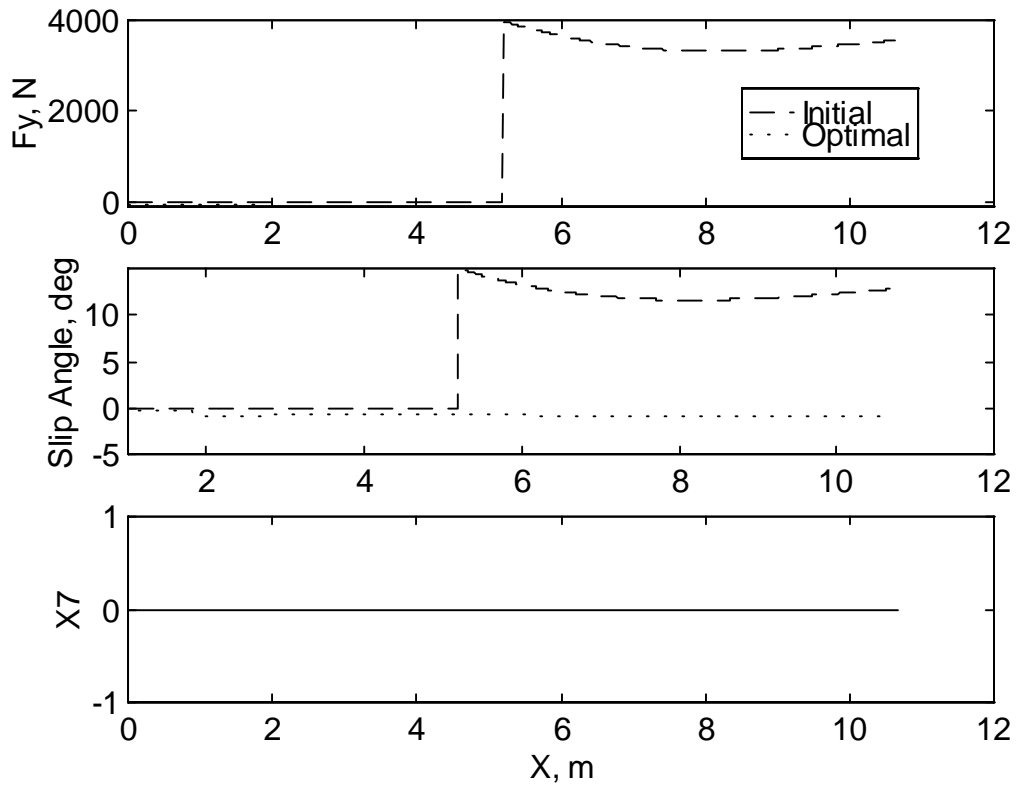


**Figure 4.14 Case No. 2: Lateral Force, Slip Angle, & Vehicle Speed Constraint**

The lateral force and the slip angle show the same trend as the steering angle. The speed constraint variable is zero for the entire path because the maximum speed of 120 mph (27.0 m/s) is not exceeded.

Figure 4.15 shows the path constraint variable, the steering angle constraint variable, and the longitudinal force constraint variable.

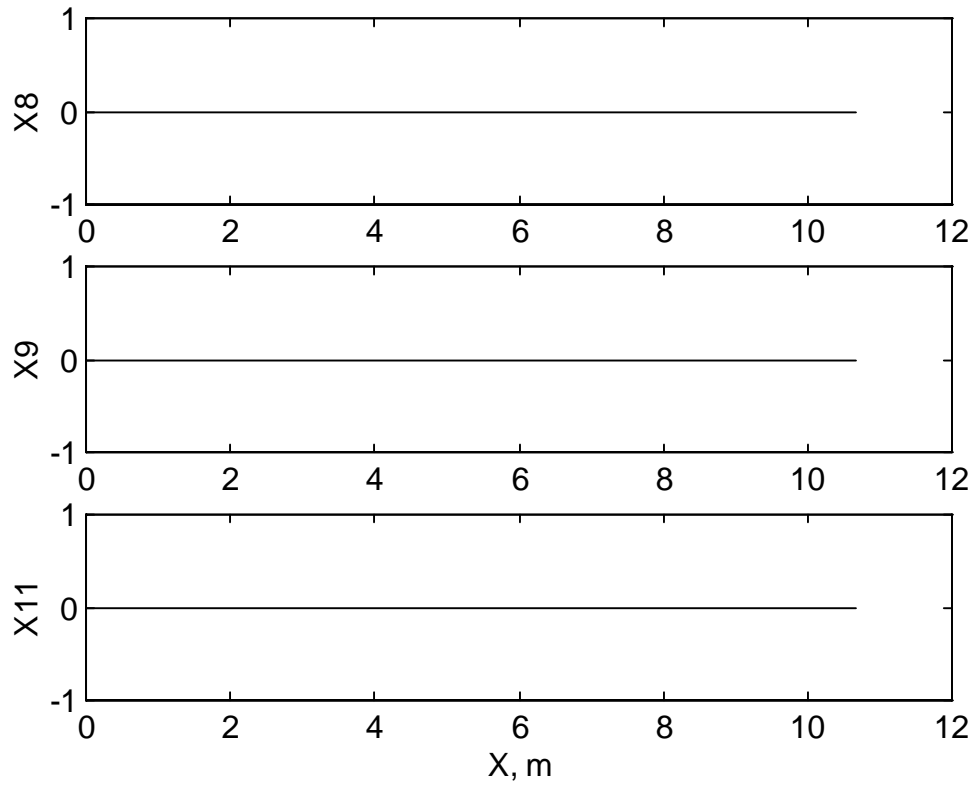


**Figure 4.15 Case No. 2: Path Constraint ( $x_8$ ), Steering Angle Constraint ( $x_9$ ), & Longitudinal Force Constraint ( $x_{11}$ )**

None of these variables exceeded the constraint condition defined in the penalty functions, Eqs. (3.8), (3.10), and (3.13) therefore their values are zero.

#### 4.4.1.2 Sine Wave Steering Angle Input

As for the sine wave steering angle input, the optimization routine is allowed to adjust the amplitude, the frequency, and the offset term of the sine wave steering input function as shown in Eq. (4.1).

$$\delta(t) = A + B \sin(2\pi Ct) \quad (4.1)$$

where

- $\delta$  = steering angle
- A = offset term
- B = sine wave amplitude
- C = sine wave frequency

A single sine wave is used for both sections of the track since there are three parameters to be optimized by the simulation algorithm associated with the input function. If two sine waves are used, a total of six variables would be required for the optimization routine to solve. A single sine wave adequately demonstrates the effectiveness of the minimum time objective algorithm. Table 4.8 shows the values of the initial system inputs for the sine wave steering angle input function.

**Table 4.8 Values of Initial System Inputs for Sine Input/Two-Section Track**

Track Section	Variable	Value
1 & 2	A	20 deg
1 & 2	B	20 deg
1 & 2	C	7 Hz
1 & 2	$P_f$	2000 N
1 & 2	t	0.5 sec

#### 4.4.1.2.1 Case No. 3: Minimum Time, $V_{\eta} = 10$ m/s, Sine Input

For Case No. 3, the system inputs are a sine wave steering angles, and a constant longitudinal force as shown in Table 4.9, which lists the initial conditions of the dynamic variables.

**Table 4.9 Case No. 3: Initial Values of Vehicle Model**

Variable	Value
$X_1$	0
$X_2$	0
$X_3$	10
$X_4$	0
$X_5$	0
$X_6$	0
$X_7$	0
$X_8$	0
$X_9$	0
$X_{10}$	0
$X_{11}$	0

Figure 4.16 shows the optimized steering angle and longitudinal force, indicated by the dotted line, plotted against the initial condition indicated by the dashed line.

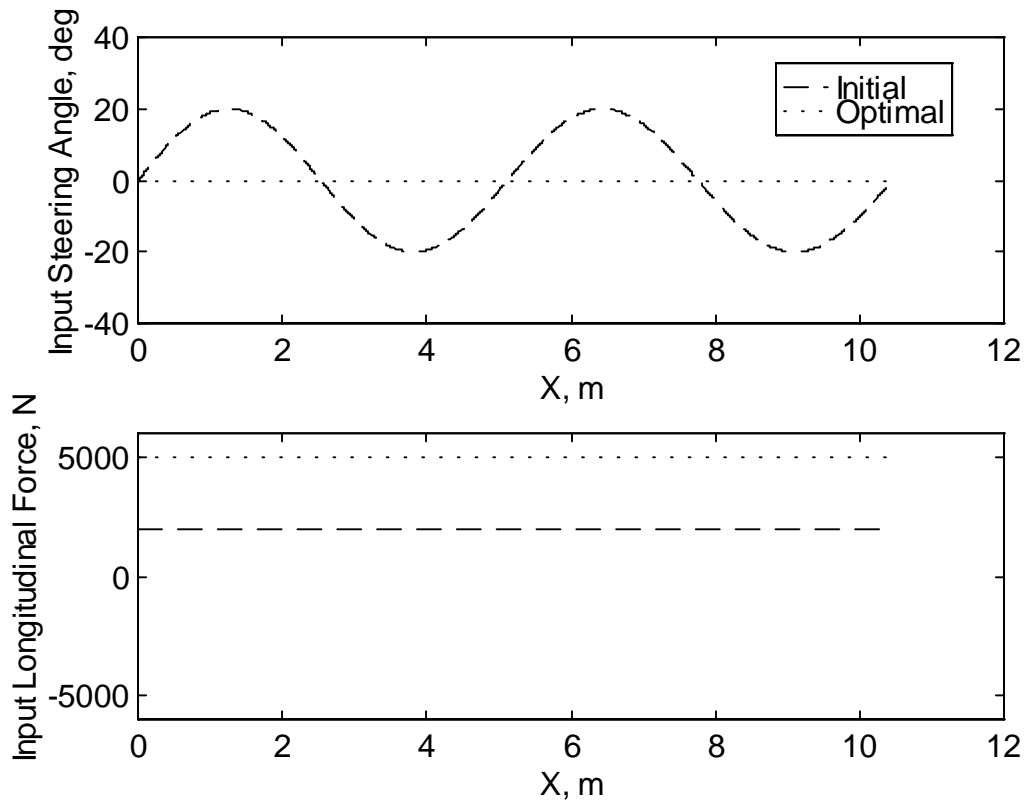


**Figure 4.16 Case No. 3 Optimal System Input**

As anticipated, the steering angle is very close to zero since the quickest path between two points the vehicle can take is a straight line while complying to the path constraint. The actual values of constants A, B, and C from Eq. (4.1) are shown in Table 4.10

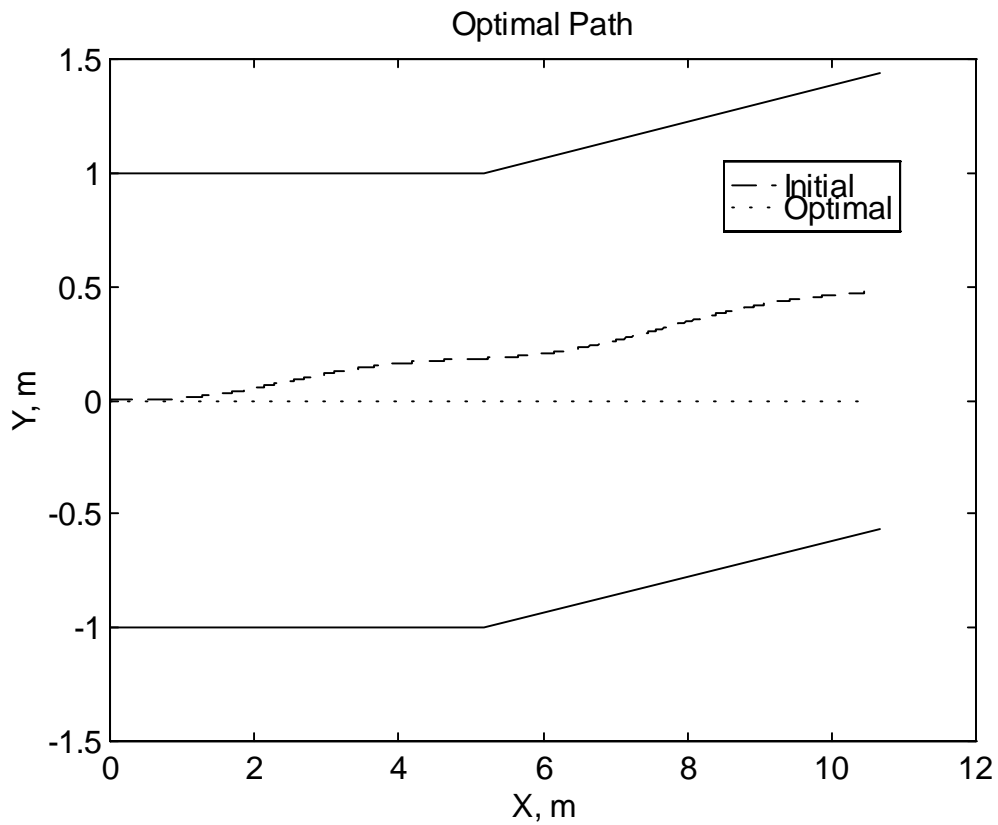
**Table 4.10 Case No. 3: Optimal Values of the Sine Wave Steering Input**

Variable	Value
A	-4.45E-6
B	6.50E-6
C	6.45E-6
t	0.890



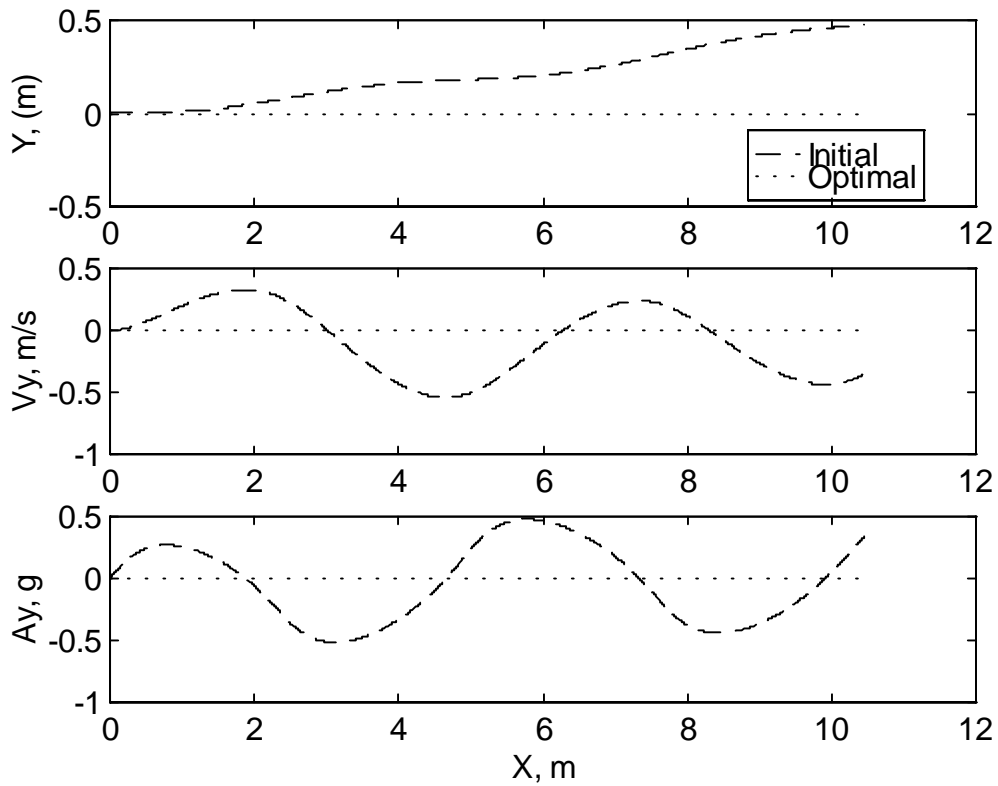
Also as anticipated, the longitudinal force is at full throttle, 5000 N, since the quickest way to get to the desired destination is full acceleration. These two optimal system inputs seem to comply with intuition.

Figure 4.17 shows the optimal path of the vehicle which can be seen that the path is very close to a straight line even with an initial steering angle input of a sine wave. This is anticipated since the quickest path between two points is a straight line.



**Figure 4.17 Case No. 3: Optimal Vehicle Path**

Figure 4.18 shows the lateral position, the lateral velocity, and the lateral acceleration of the vehicle at the optimal condition.



**Figure 4.18 Case No. 3: Lateral Position, Lateral Velocity, & Lateral Acceleration**

All these variables are very close to zero corresponding the steering input being very close to zero.

Figure 4.19 shows the longitudinal velocity, the yaw angle, and the yaw velocity of the vehicle at the optimal condition.

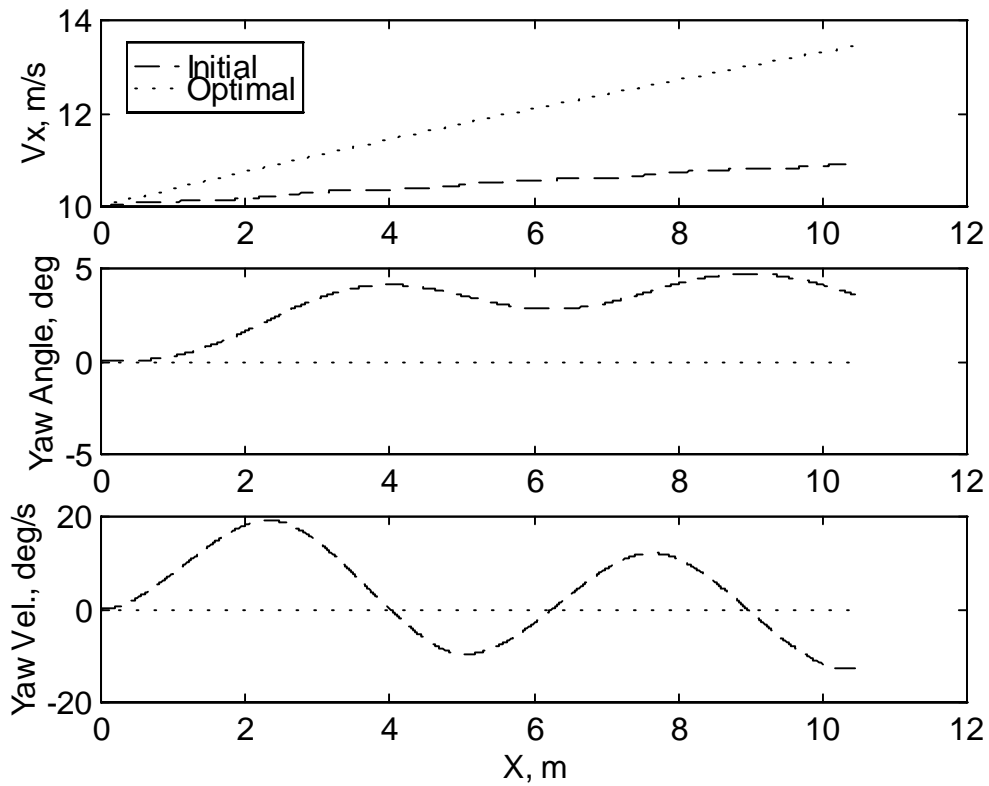


**Figure 4.19 Case No. 3: Longitudinal Velocity, Yaw Angle, & Yaw Velocity**

The longitudinal velocity shows a steady increase since the longitudinal force applied to the vehicle is constant at full throttle for the entire path. The yaw angle and the yaw velocity are very close to zero, again corresponding the optimal steering angle being very close to zero.

Figure 4.20 shows the optimal lateral force, the slip angle, and the speed constraint condition.

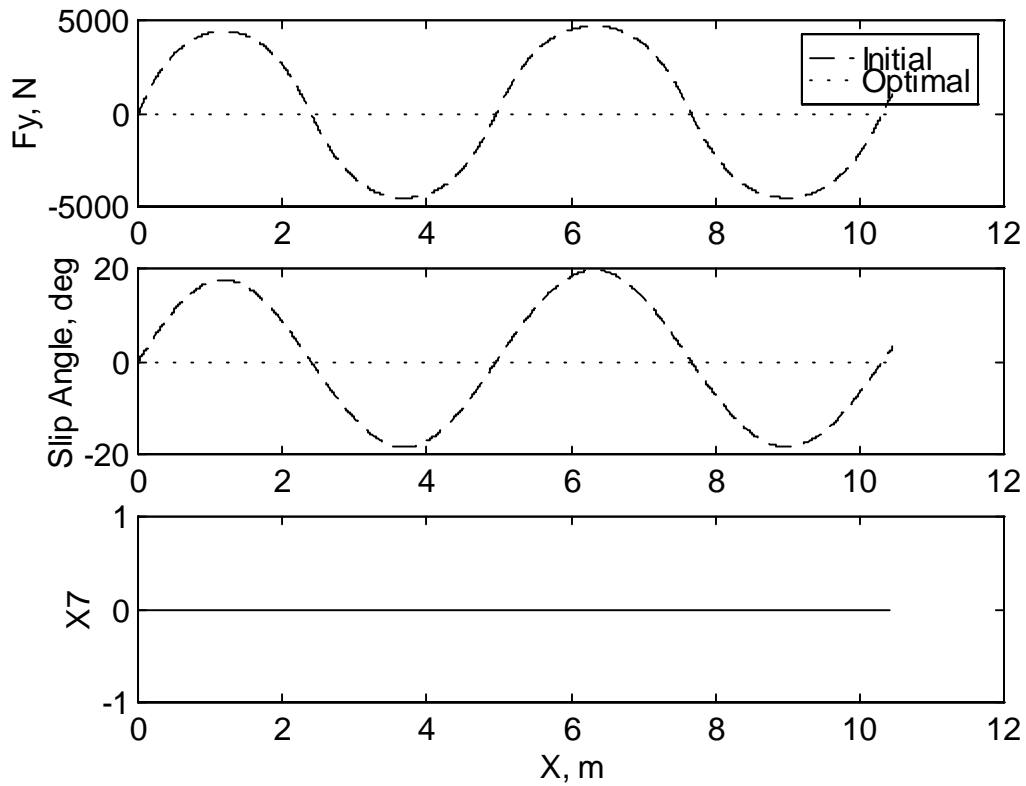


**Figure 4.20 Case No. 3: Lateral Force, Slip Angle, & Vehicle Speed Constraint**

The lateral force and the slip angle are very close to zero corresponding to the fact that the optimal steering angle is very close to zero. The speed constraint variable is zero for the entire path because the maximum speed of 120 mph (27.0 m/s) is not exceeded.

Figure 4.21 shows the path constraint variable, the steering angle constraint variable, and the longitudinal force constraint variable.

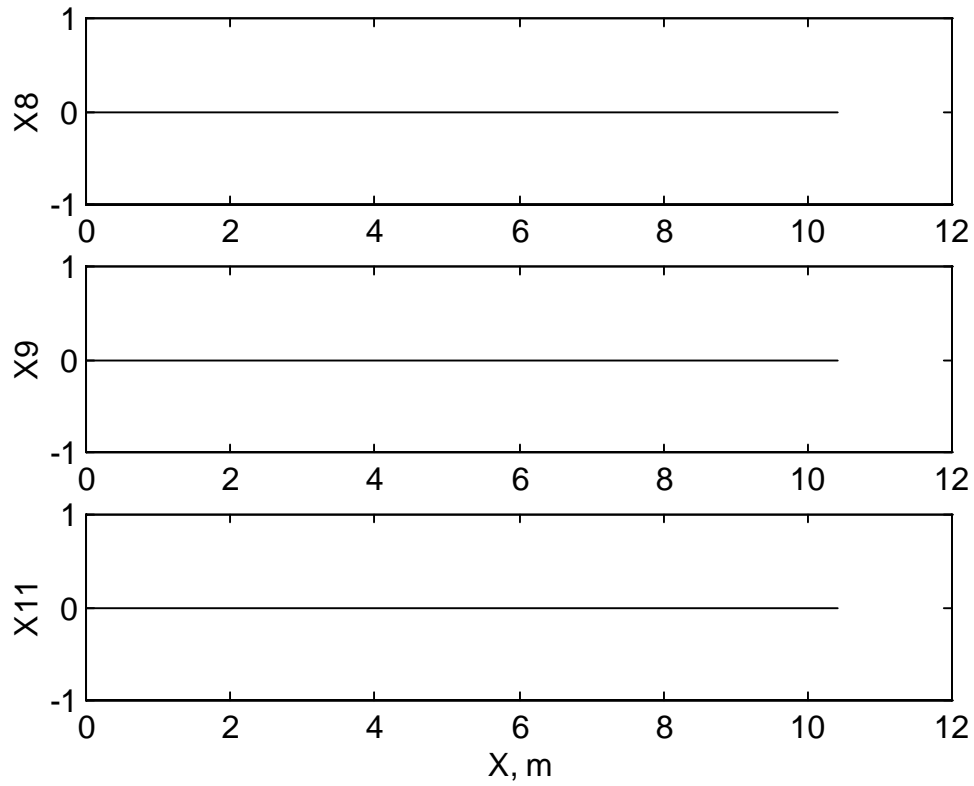


**Figure 4.21 Case No. 3: Path Constraint ( $x_8$ ), Steering Angle Constraint ( $x_9$ ), & Longitudinal Force Constraint ( $x_{11}$ )**

None of these variables exceeded the constraint condition defined in the penalty functions, Eqs. (3.8), (3.10), and (3.13).

## 4.4.2 Three-Section Test Track

Figure 4.22 shows the three-section test track used for this particular simulation.

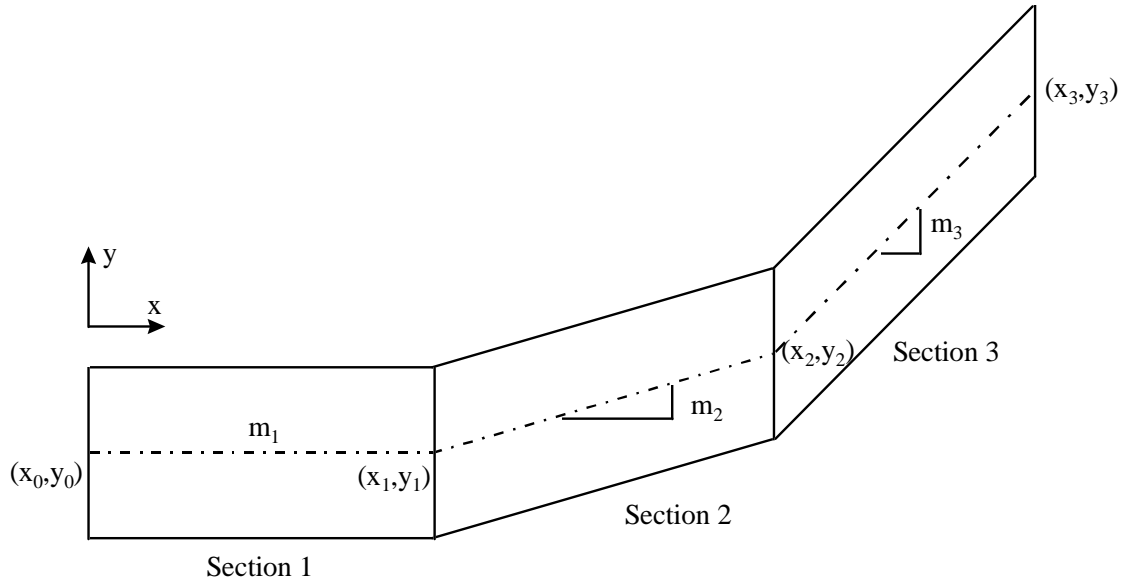


**Figure 4.22 Three-Section Test Track**

Table 4.11 lists the coordinates and the slopes of the track.

**Table 4.11 Three-Section Test Track Specifications**

Track Section	X end position (m)	Y end position (m)	Slope
1	5.194	0.307	0.597
2	10.143	1.732	0.285
3	14.822	4.064	0.498

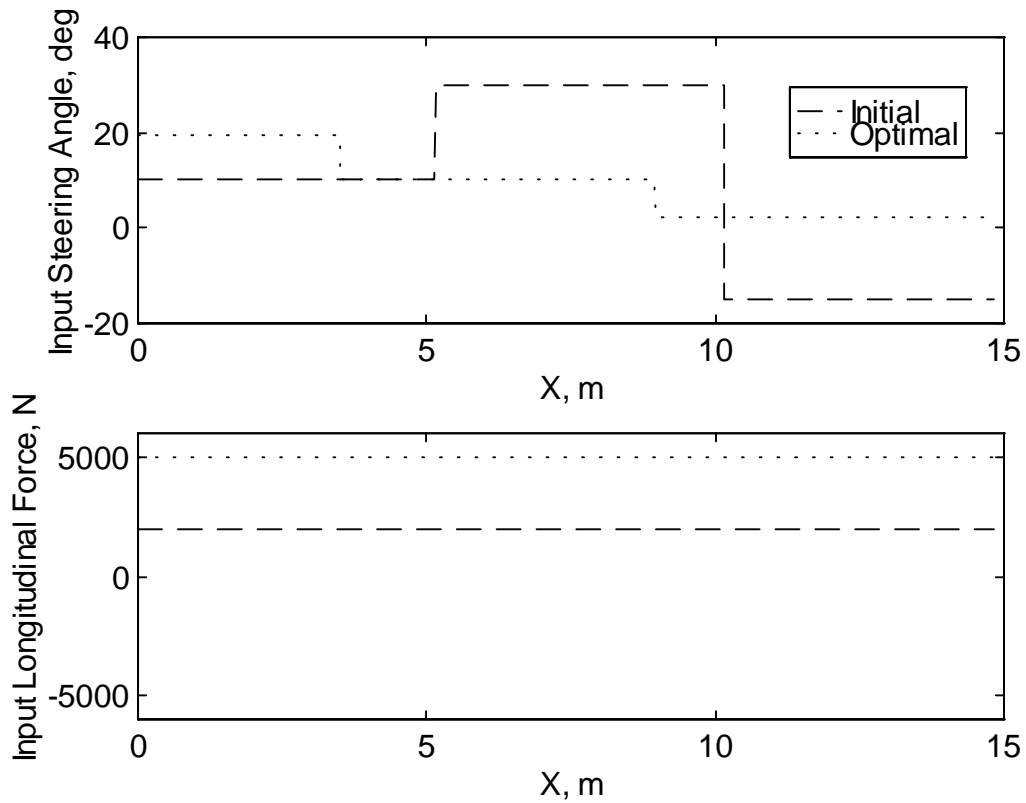
#### 4.4.2.1 Case No. 4: Minimum Time, $V_{\eta} = 10$ m/s, Step Input

Table 4.12 lists the initial conditions of the dynamic variables.

**Table 4.12 Case No. 4: Initial Values of Step/Three-Section Track Simulation**

Variable	Value
$X_1$	0
$X_2$	0
$X_3$	10
$X_4$	0
$X_5$	0
$X_6$	0
$X_7$	0
$X_8$	0
$X_9$	0
$X_{10}$	0
$X_{11}$	0

Figure 4.23 shows the optimized steering angle and longitudinal force, indicated by the dotted line, plotted against the initial condition indicated by the dashed line.



**Figure 4.23 Case No. 4 Optimal System Input**

As anticipated, the steering angle is very close to zero since the quickest path the vehicle can take is a straight line while complying to the path constraint. Also as anticipated, the longitudinal force is at full throttle, 5000 N, since the quickest way to get to the desired destination is full acceleration. These two optimal system inputs seem to comply with intuition.

Table 4.13 lists the values of the optimal system input variables and time.



**Table 4.13 Values of Optimal System Inputs for Step Input/Three-Section Track**

Track Section	Variable	Value
1	$\delta$	19.367 deg
	$P_f$	5000 N
	t	0.333 sec
2	$\delta$	10.056 deg
	$P_f$	5000 N
	t	0.464 sec.
3	$\delta$	2.126 deg
	$P_f$	5000 N
	t	0.455 sec

where

$\delta$  = steering angle

$P_f$  = longitudinal force

t = time

The execution time of the first track section actually increased by 8.8% to 0.544 sec. However, the second section of the track has a significant reduction, 27.8% to 0.361 sec. Therefore it can be seen that the minimum time objective has been met by the optimization algorithm with a total reduction in execution time of 9.5% to 0.905 sec.

Figure 4.24 shows the optimal path of the vehicle, which can be seen, the path is very close to a straight line.

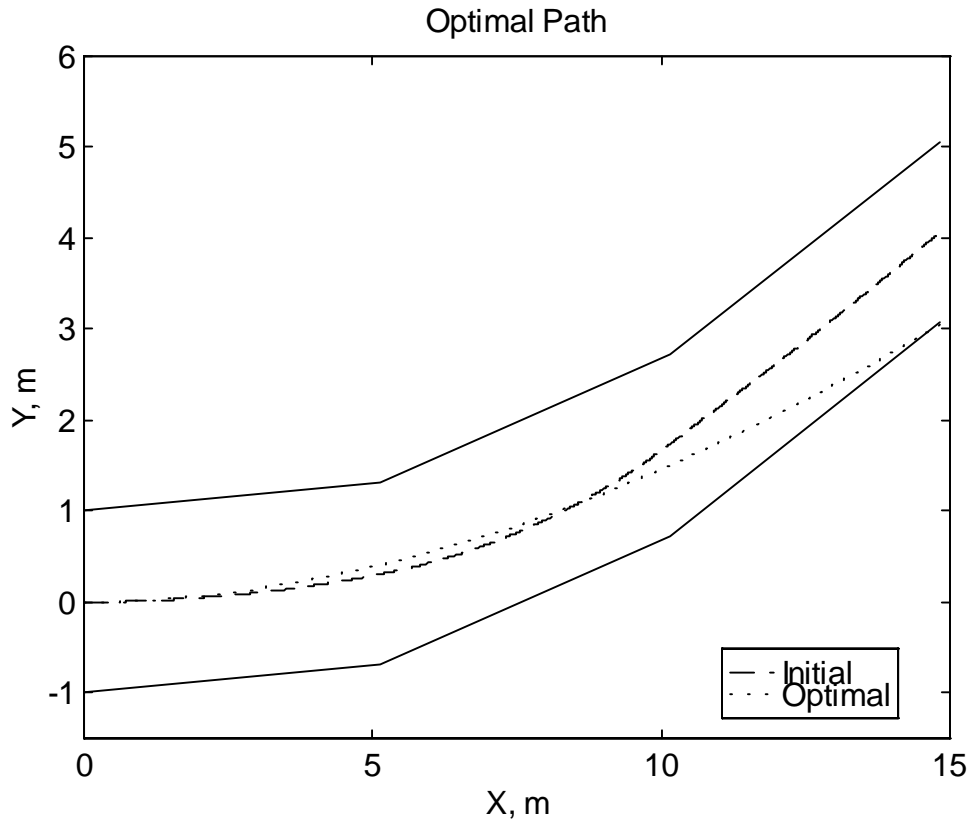


**Figure 4.24 Case No. 4 Optimal Vehicle Path**

This is anticipated since the quickest path between two points is a straight line.

Figure 4.25 shows the lateral position, the lateral velocity, and the lateral acceleration of the vehicle at the optimal condition.

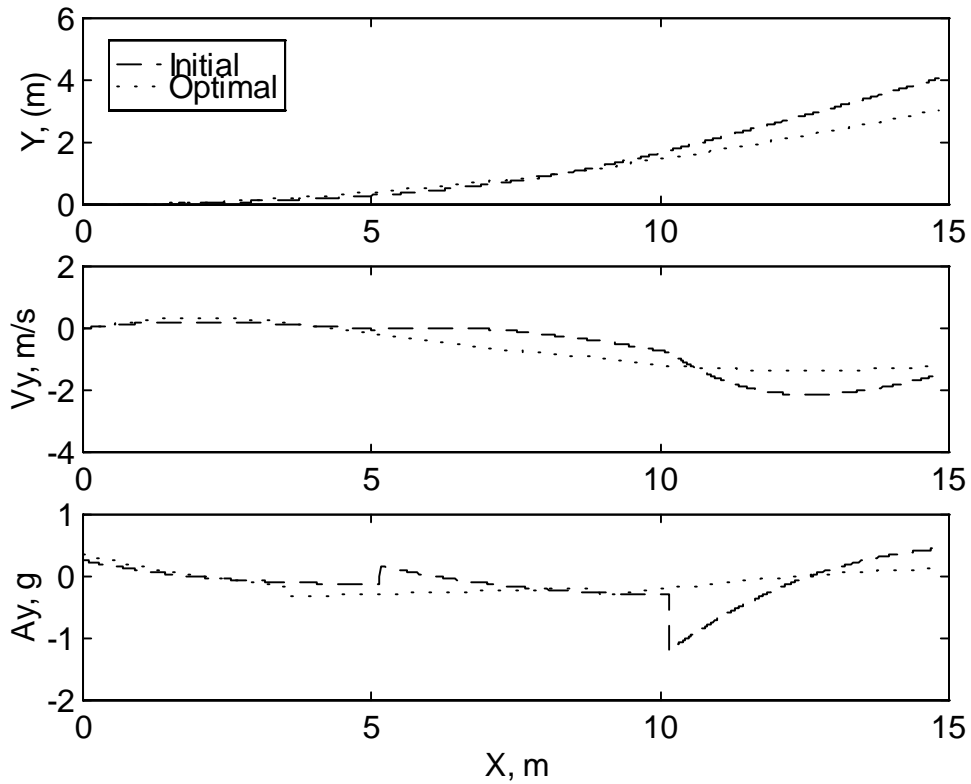


**Figure 4.25 Case No. 4: Lateral Position, Lateral Velocity, & Lateral Acceleration**

Both optimal lateral velocity and acceleration show less amplitudes compare to the initial values. This shows that the vehicle is trying to pursue a more straight path, with less lateral motion, which in effect trying to minimize time.

Figure 4.26 shows the longitudinal velocity, the yaw angle, and the yaw velocity of the vehicle at the optimal condition.

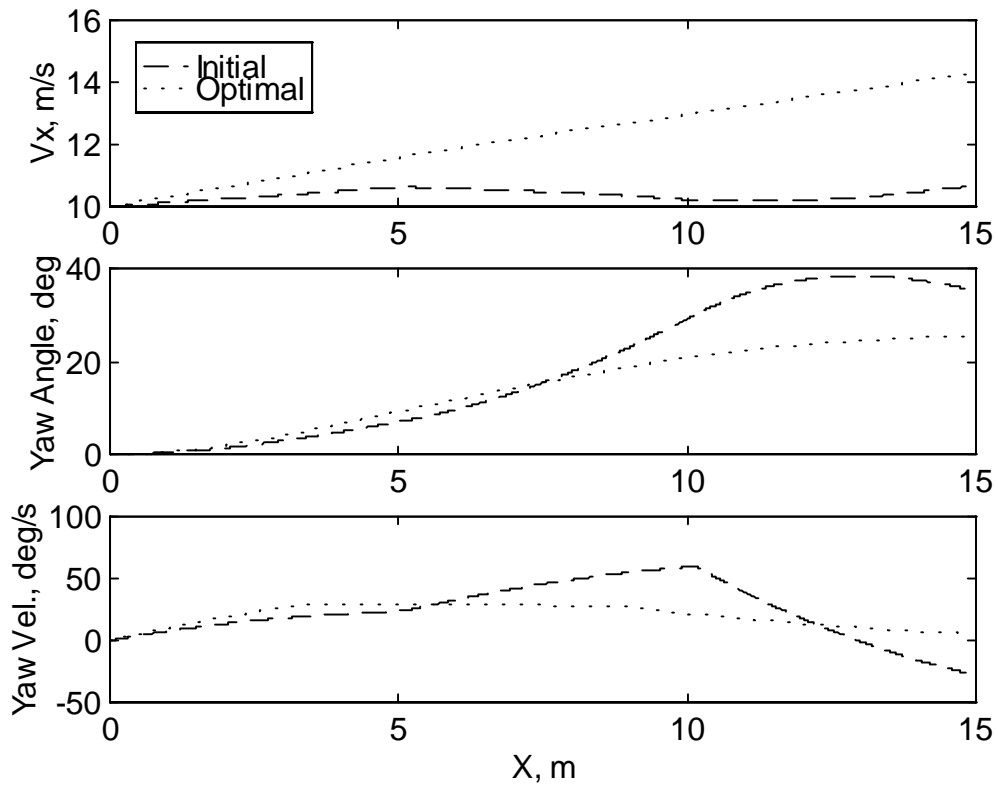


**Figure 4.26 Case No. 4: Longitudinal Velocity, Yaw Angle, & Yaw Velocity**

The longitudinal velocity shows a steady increase since the longitudinal force applied to the vehicle is constant at full throttle for the entire path. The optimal yaw angle and velocity are showing less motion compare to the initial response. Again, this is due to the fact that less yaw motion is required for the vehicle to reach its desired trajectory in minimum time.

Figure 4.27 shows the optimal lateral force, the slip angle, and the speed constraint condition.

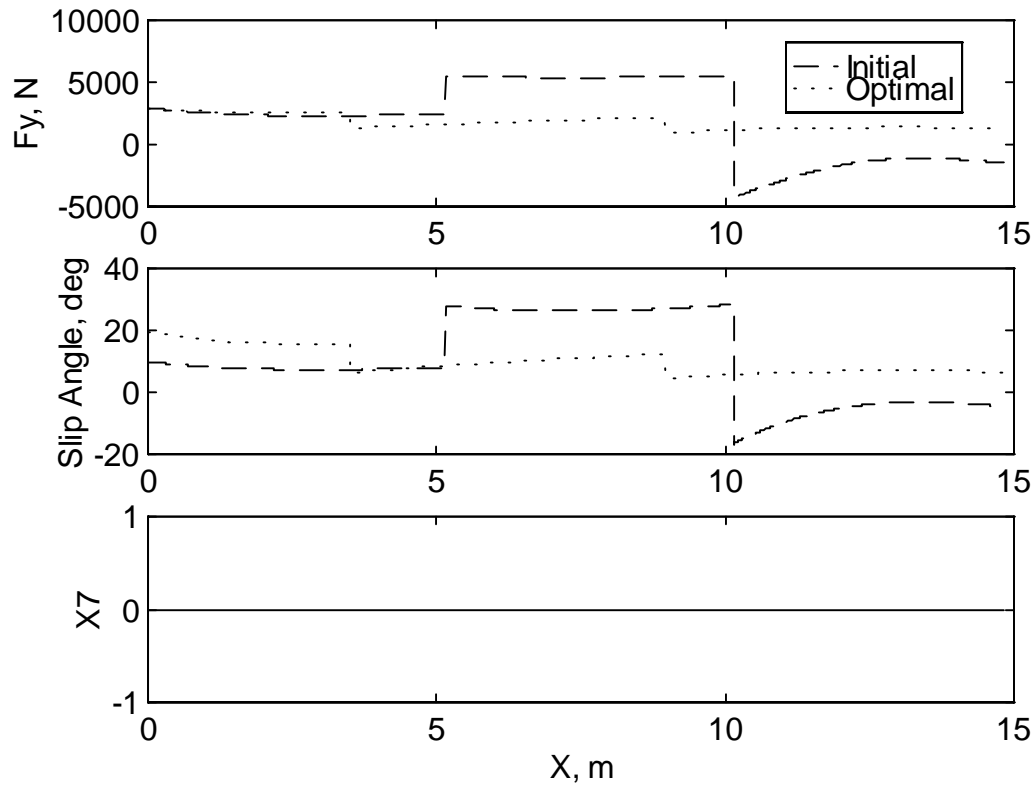


**Figure 4.27 Case No. 4: Lateral Force, Slip Angle, & Vehicle Speed Constraint**

The lateral force and the slip angle show the same point, emphasizing the effectiveness of the optimization algorithm, and showing that the vehicle is going through less lateral motion to satisfy the minimum time objective. The speed constraint variable is zero for the entire path because the maximum speed of 120 mph (27.0 m/s) is not exceeded.

Figure 4.28 shows the path constraint variable, the steering angle constraint variable, and the longitudinal force constraint variable.

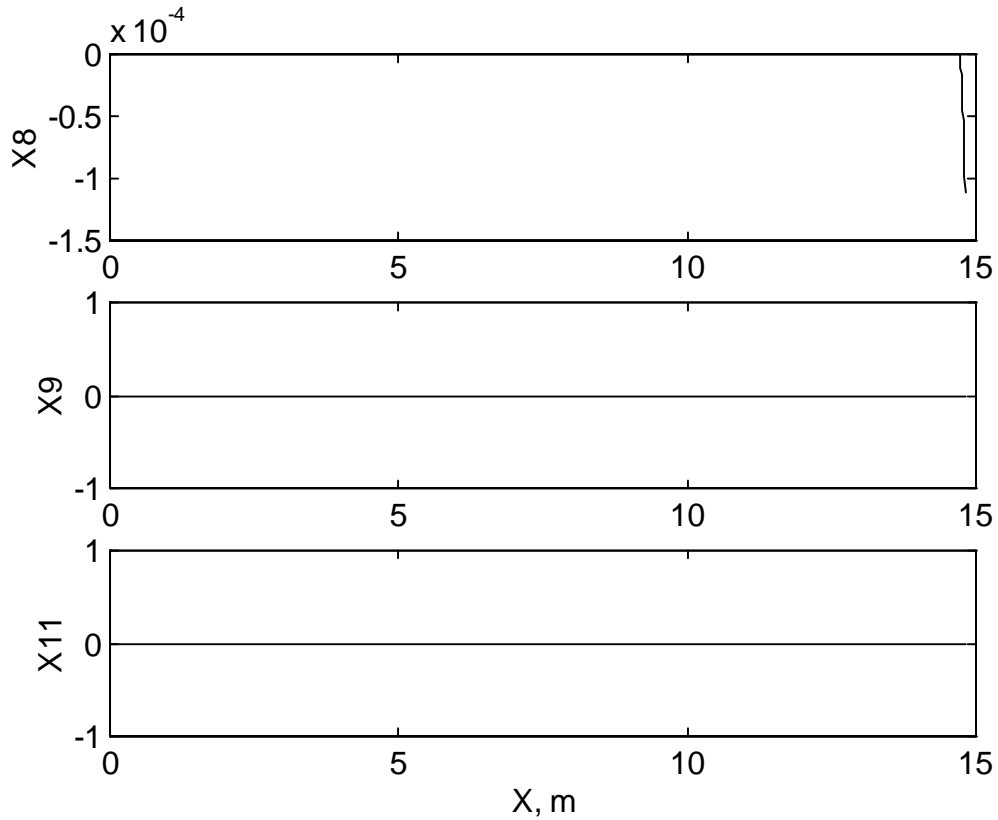


**Figure 4.28 Case No. 4: Path Constraint ( $x_8$ ), Steering Angle Constraint ( $x_9$ ), & Longitudinal Force Constraint ( $x_{11}$ )**

None of these variables exceeded the constraint condition defined in the penalty functions, Eqs. (3.8), (3.10), and (3.13) except for the path constraint. There exists a very small violation at the very end of the path. However, the error is so small that this value can be ignored.

## 4.5 Maximize Tire Forces

The objective of this simulation is to determine the optimal path that would maximize tire forces of the vehicle. Four cases are simulated to demonstrate the effectiveness of the optimization algorithm and to show that idea of optimization could be used to determine an optimal path satisfying the objective function, Eq. (3.16). Essentially the total tire force for the vehicle to get to the desired position is evaluated for each case. It is believed to be maximized due to the fact that the scalar value of the cost function is minimized.

### 4.5.1.1 Case No. 5: Max. Tire Force, $V_{\eta} = 10$ m/s, Step Input

For Case No. 5, the system inputs are a series of step steering angles, and a constant longitudinal force as shown in Table 4.14, which lists the initial conditions of the dynamic variables.

**Table 4.14 Case No. 5: Initial Values of Step/Two-Section Track Simulation**

Variable	Value
$X_1$	0
$X_2$	0
$X_3$	10
$X_4$	0
$X_5$	0
$X_6$	0
$X_7$	0
$X_8$	0
$X_9$	0
$X_{10}$	0
$X_{11}$	0

These values were selected so the initial response of the vehicle would be moderated and the vehicle would stay within the boundaries of the track.

Figure 4.29 shows the optimized steering angle and longitudinal force, indicated by the dotted line, plotted against the initial condition indicated by the dashed line.

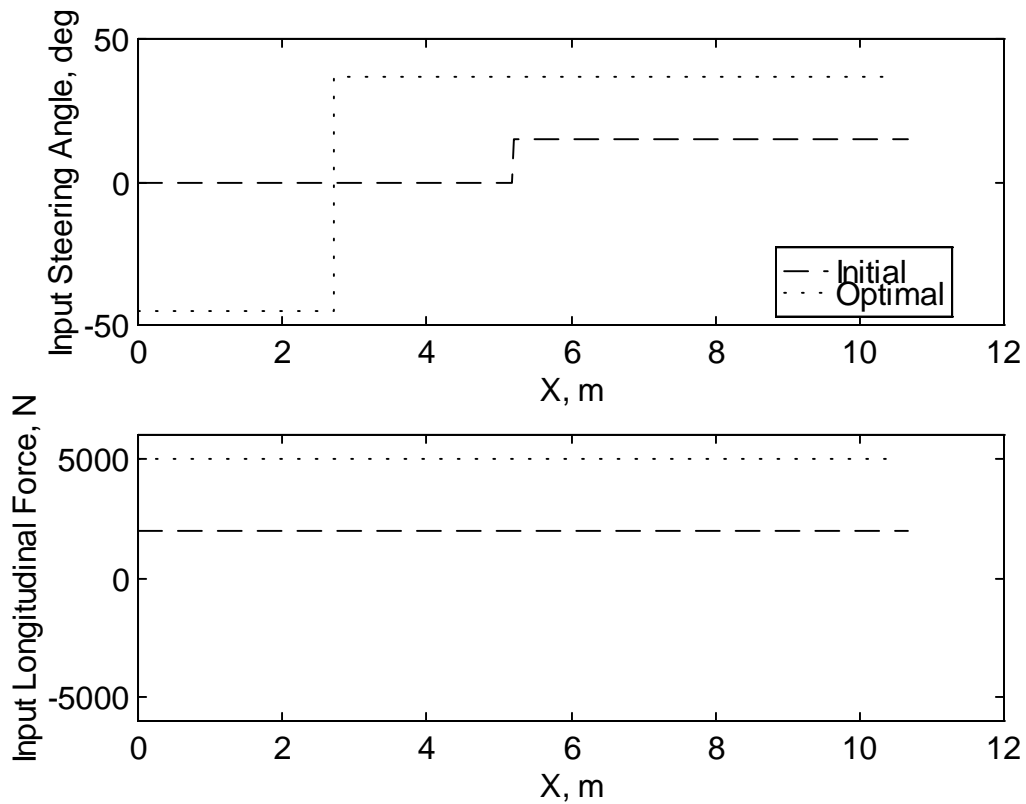


**Figure 4.29 Case No. 5 Optimal System Input**

As anticipated, the optimal steering angle input goes to extreme values to obtain maximum tire forces. The longitudinal force of the tire is optimized to be at full throttle for the entire path. These two optimal system inputs seem to comply with intuition.

Table 4.15 lists the values of the optimal system input variables and time.



**Table 4.15 Values of Optimal System Inputs for Step Input/Two-Section Track**

Track Section	Variable	Value
1	$\delta$	-45 deg
	$P_f$	5000 N
	t	0.266 sec
2	$\delta$	37.05 deg
	$P_f$	5000 N
	t	0.683 sec.

where

$\delta$  = steering angle

$P_f$  = longitudinal force

t = time

The execution time of the first track section actually increased by 8.8% to 0.544 sec. However, the second section of the track has a significant reduction, 27.8% to 0.361 sec. Therefore it can be seen that the minimum time objective has been met by the optimization algorithm with a total reduction in execution time of 9.5% to 0.905 sec.

Figure 4.30 shows that the optimal path is more extreme than the initial path of the vehicle.

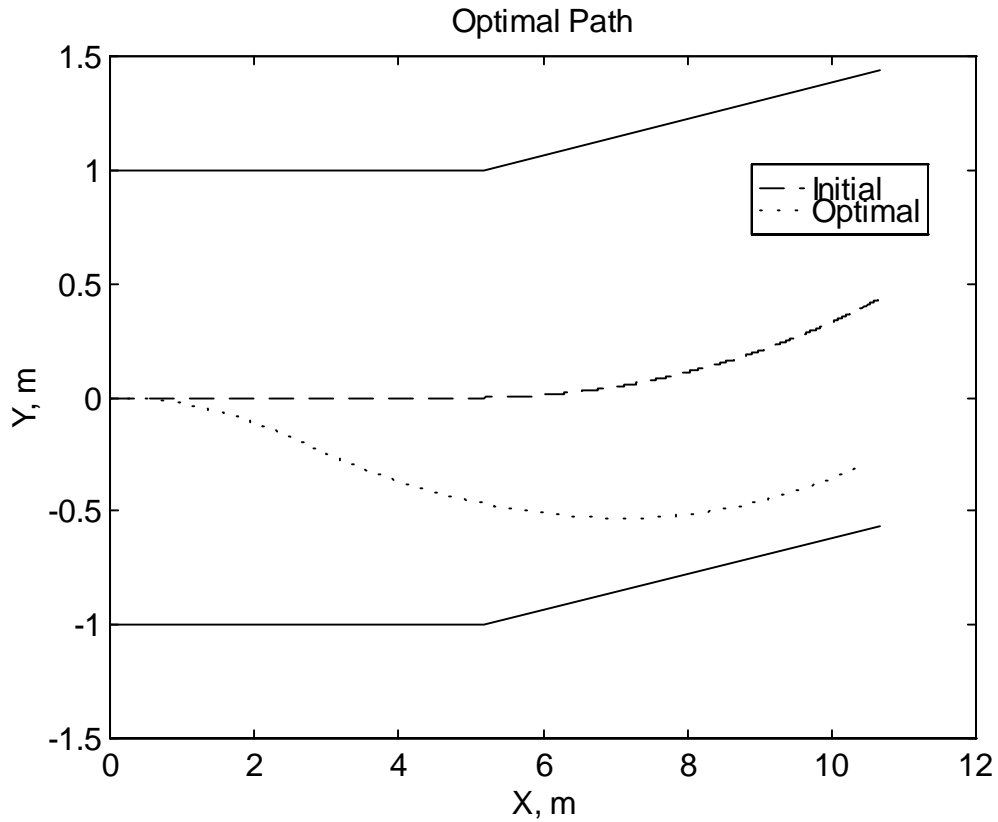


**Figure 4.30 Case No. 5 Optimal Vehicle Path**

This is understandable since the vehicle needs to generate high lateral force, which is a function of slip angle. These variables will be described later.

Figure 4.31 shows the lateral position, the lateral velocity, and the lateral acceleration of the vehicle at the optimal condition.

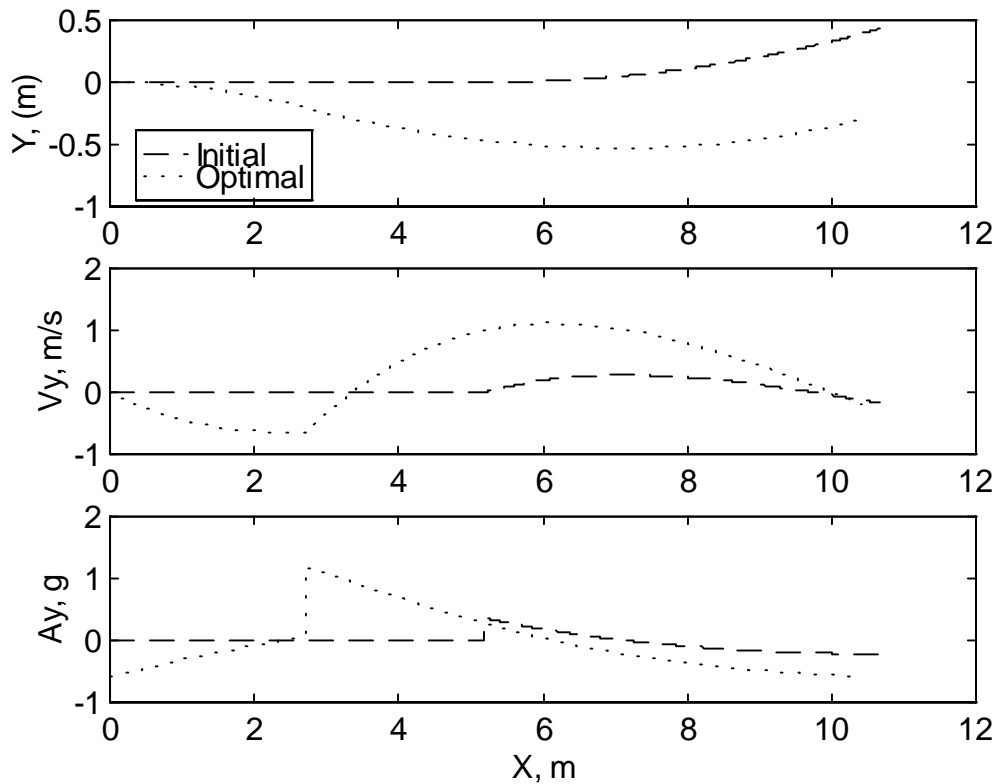


**Figure 4.31 Case No. 5: Lateral Position, Lateral Velocity, & Lateral Acceleration**

All the variables show larger lateral motion of the vehicle with respect to the initial response. This is the opposite of the minimum time objective where the lateral motion is conserved so time is not wasted. Here tires are subjected to perform more work at extreme condition.

Figure 4.32 shows the longitudinal velocity, the yaw angle, and the yaw velocity of the vehicle at the optimal condition.

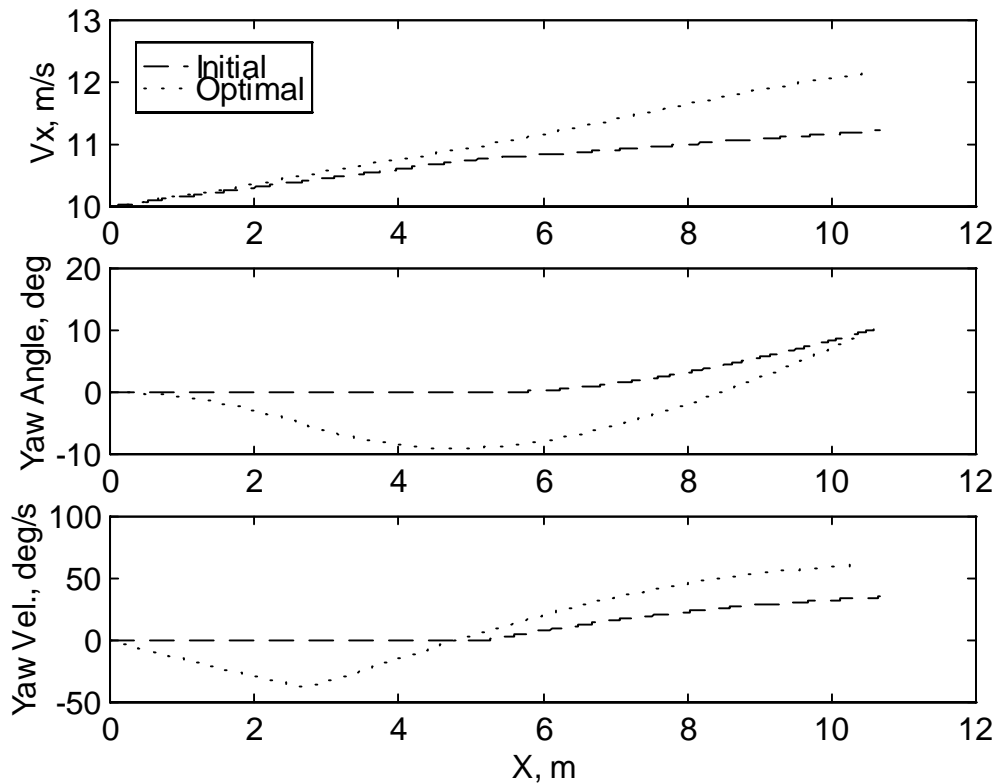


**Figure 4.32 Case No. 5: Longitudinal Velocity, Yaw Angle, & Yaw Velocity**

The longitudinal velocity shows a steady increase since the longitudinal force applied to the vehicle is constant at full throttle for the entire path. The optimal yaw angle and velocity demonstrate the fact that while the vehicle is subjected to higher lateral motion, higher yaw motion is also experienced. These values are higher than the initial response in trying to satisfy the objective function.

Figure 4.33 shows the optimal lateral force, the slip angle, and the speed constraint condition.

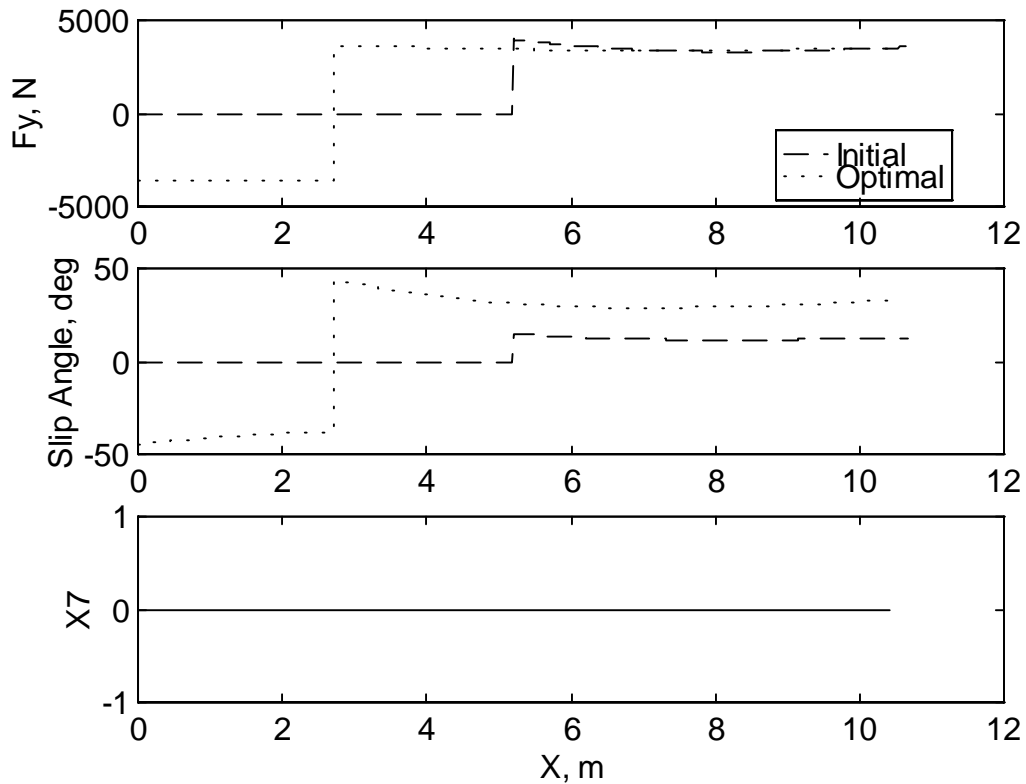


**Figure 4.33 Case No. 5: Lateral Force, Slip Angle, & Vehicle Speed Constraint**

The optimal condition generates higher lateral force in trying to meet the objective function. It doesn't matter whether the value of the lateral force is positive or negative as long as the magnitude is maximized, the objective is satisfied. The optimal slip angle shows the same trend as the lateral force. The speed constraint variable is zero for the entire path because the maximum speed of 120 mph (27.0 m/s) is not exceeded.

Figure 4.34 shows the path constraint variable, the steering angle constraint variable, and the longitudinal force constraint variable.

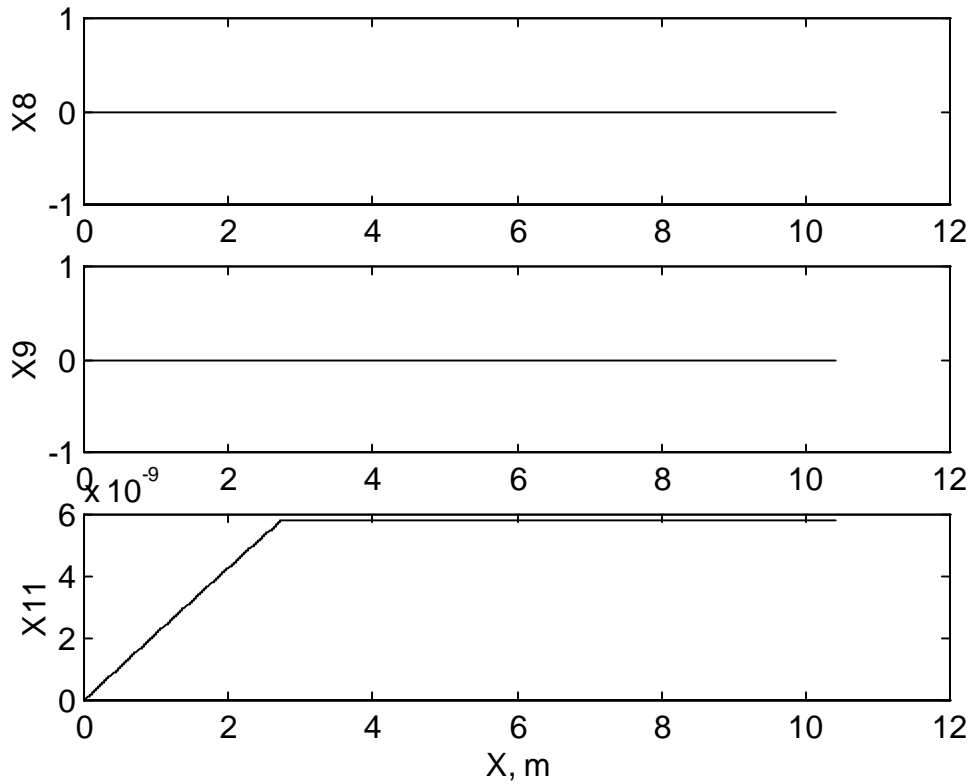


**Figure 4.34 Case No. 5: Path Constraint ( $x_8$ ), Steering Angle Constraint ( $x_9$ ), & Longitudinal Force Constraint ( $x_{11}$ )**

In fact the longitudinal force exceeded the constraint set by Eq. (3.10), however, the algorithm is setup so that the input longitudinal force is saturated for any value above the operating range defined in Eq. (3.9). Therefore any longitudinal force value higher than the saturation force is seen by the vehicle, instead the saturation force is used instead. None of other variables exceeded the constraint condition defined in the penalty functions, Eqs. (3.8), (3.10), and (3.13).

Figure 4.35 shows the augmented state variable describing the maximizing of tire forces function, described in Eq. (3.15), and the resultant tire force.

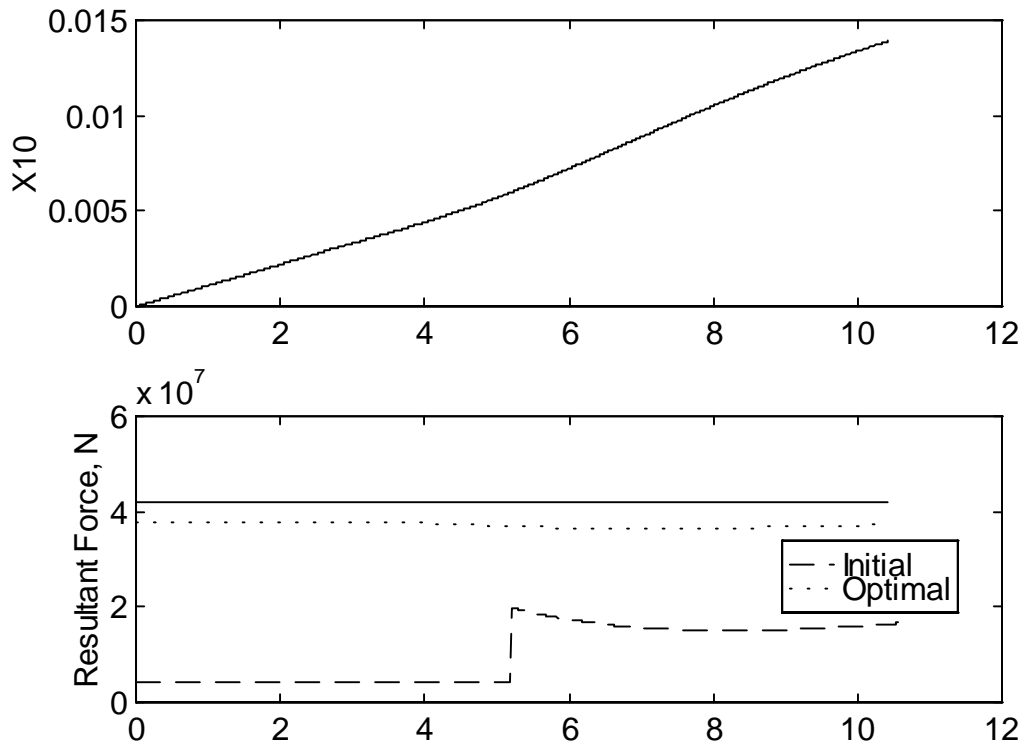


**Figure 4.35 Case No. 5: Maximize Tire Forces Objective Variable, Resultant Force**

The optimal resultant force is close to the maximum allowable as shown above, however, the tire force objective variable,  $x_{10}$ , indicates its error squared.

### 4.5.1.2 Case No. 6: Max. Tire Force, $V_{\eta} = 20$ m/s, Step Input

For Case No. 6, the system inputs are a series of step steering angles, and a constant longitudinal force as shown in Figure 4.36.

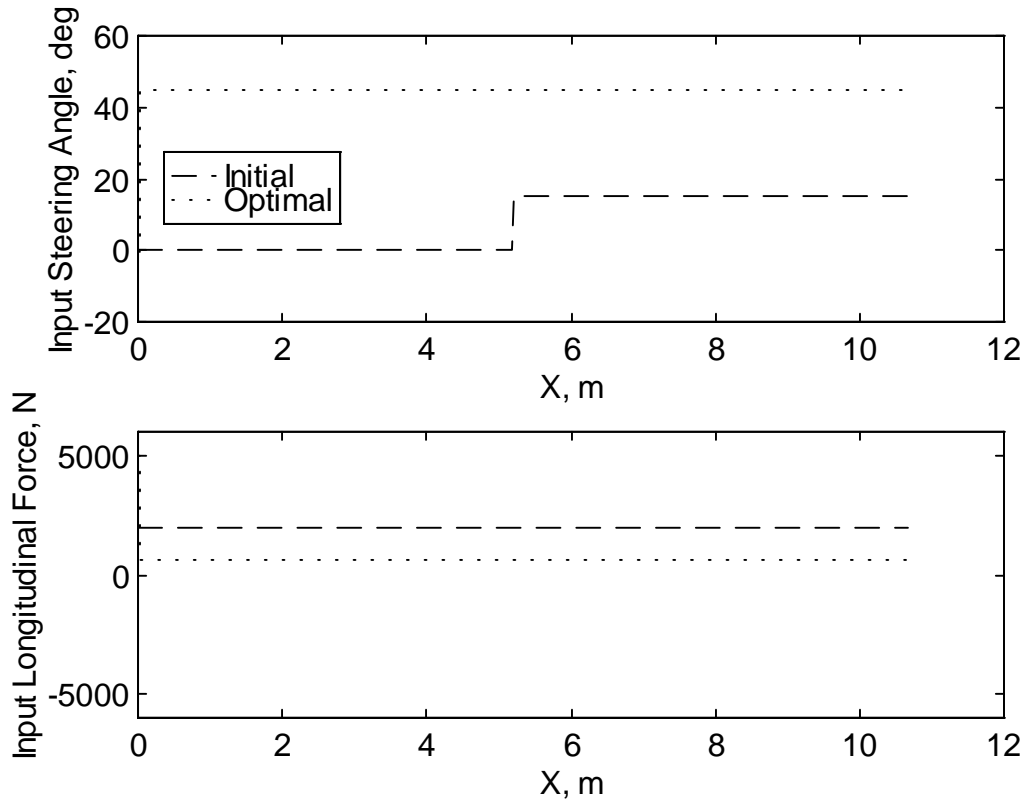


**Figure 4.36 Case No. 6 Optimal System Input**

These values were selected so the initial response of the vehicle would be moderated and the vehicle would stay within the boundaries of the track. Table 4.16 lists the initial conditions of the state variables.



**Table 4.16 Case No. 6: Initial Values of Step/Two-Section Track Simulation**

Variable	Value
$X_1$	0
$X_2$	0
$X_3$	10
$X_4$	0
$X_5$	0
$X_6$	0
$X_7$	0
$X_8$	0
$X_9$	0
$X_{10}$	0
$X_{11}$	0

Figure 4.36 also shows the optimized steering angle and longitudinal force. As anticipated, the steering angle is very close to zero since the quickest path the vehicle can take is a straight line while complying to the path constraint. Surprisingly, the longitudinal force is not at its maximum allowable, 5000 N, but rather at about 647.1 N. The optimization routine chooses to optimize on the lateral force by inputting large steering angle. Even though this is the case, the resulting tire force is still maximized by the optimization routine which will be seen later in this section.

Table 4.17 lists the values of the optimal system input variables and time.

**Table 4.17 Values of Optimal System Inputs for Step Input/Two-Section Track**

Track Section	Variable	Value
1	$\delta$	-0.115 deg
	$P_f$	5000 N
	t	0.001 sec
2	$\delta$	45.0 deg
	$P_f$	647.1 N
	t	0.562 sec.

where

$\delta$  = steering angle

$P_f$  = longitudinal force

t = time

With an initial velocity of 20 m/s, the optimization algorithm searched for a variable that could be minimized such that the scalar value of the cost function would decrease. It is suspected that the first execution time variable is driven to zero so that the vehicle could meet the final position constraint, as defined in Eq. (3.13). This is acceptable because the overall response of the vehicle still meets the objective. The total time for the optimal path resulted to be 44% less than the initial. Such a significant reduction is credited to the initial velocity of 20 m/s. The optimal longitudinal force turned out to be lower than the initial condition. The algorithm maximized on the lateral force by forcing the steering angle to its maximum, thus satisfying the objective function.

Figure 4.37 shows the optimal path of the vehicle, indicated by the dotted line, plotted against the initial condition indicated by the dashed line.

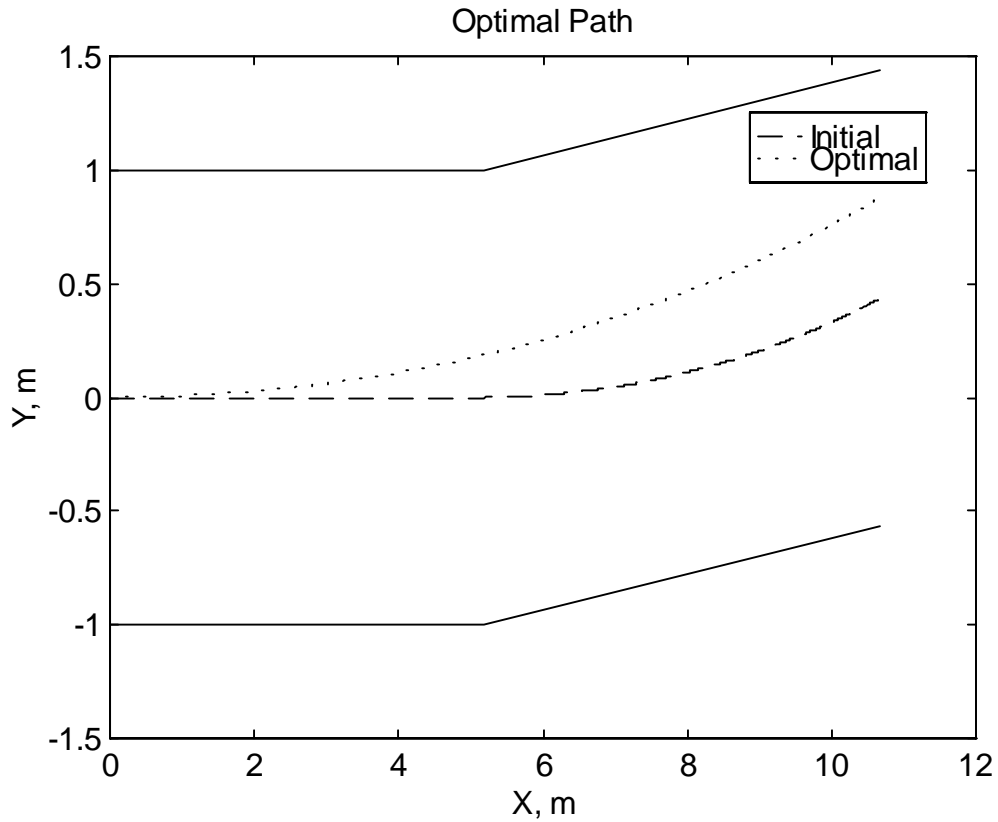


**Figure 4.37 Case No. 6 Optimal Vehicle Path**

The optimal path has more curvature from the very beginning of the path as opposed to a straight line and then a curve like the initial path. This way, front tire force is maximized for the entire path rather than a section of it.

Figure 4.38 shows the lateral position, the lateral velocity, and the lateral acceleration of the vehicle at the optimal condition.

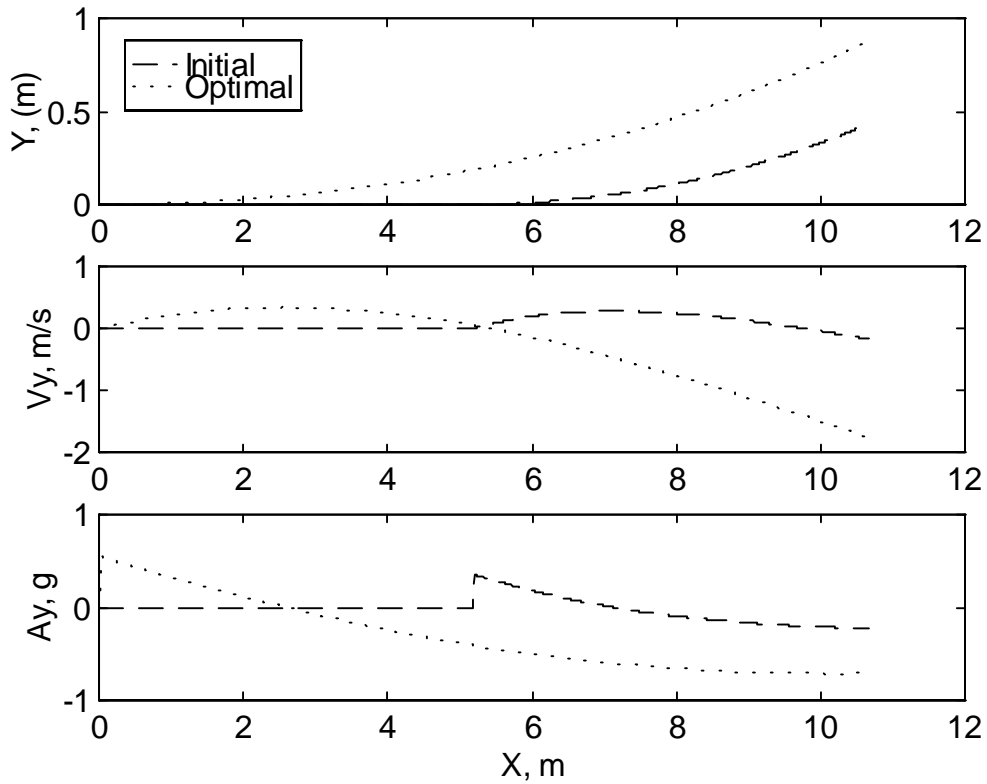


**Figure 4.38 Case No. 6: Lateral Position, Lateral Velocity, & Lateral Acceleration**

The lateral position, velocity and acceleration all demonstrate larger lateral amplitudes than the initial condition contributing to maximizing the lateral tire force.

Figure 4.39 shows the longitudinal velocity, the yaw angle, and the yaw velocity of the vehicle at the optimal condition.

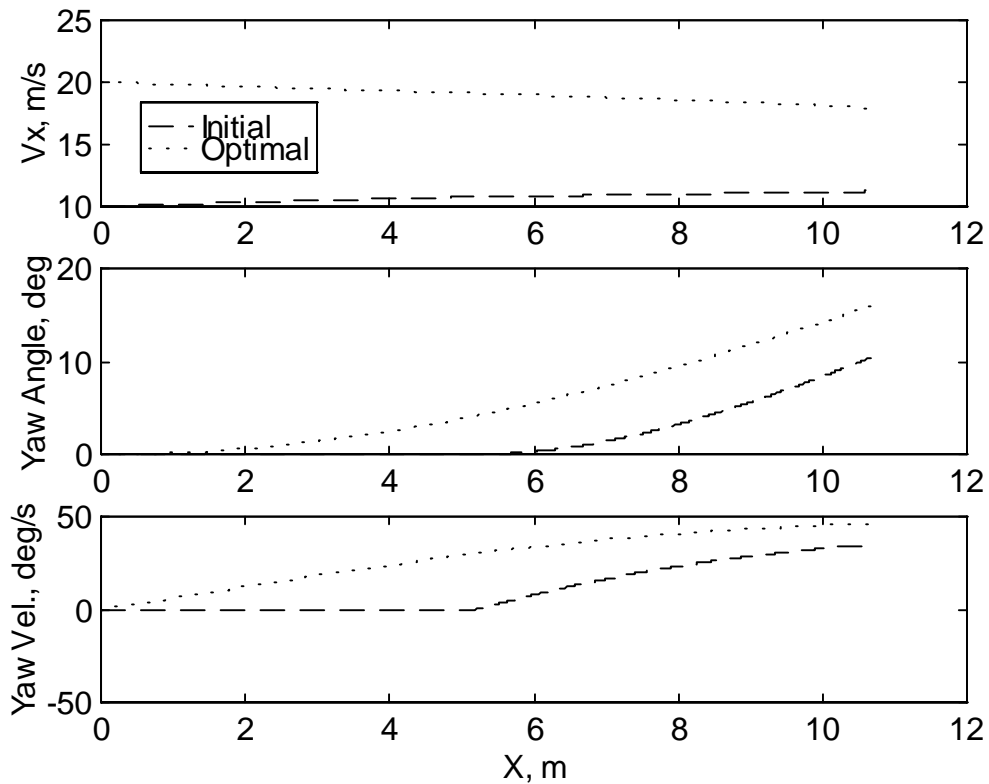


**Figure 4.39 Case No. 6: Longitudinal Velocity, Yaw Angle, & Yaw Velocity**

The longitudinal velocity shows a steady decrease from beginning to end due to the fact that the optimal longitudinal force input is low and constant. The same effect was seen in the steering symmetry validation when zero longitudinal force was used where large lateral motion with small longitudinal could actually decrease the longitudinal velocity of the vehicle. As for the optimal yaw angle and velocity, they have larger amplitudes due to the fact that there is larger steering angle input.

Figure 4.40 shows the optimal lateral force, the slip angle, and the speed constraint condition.

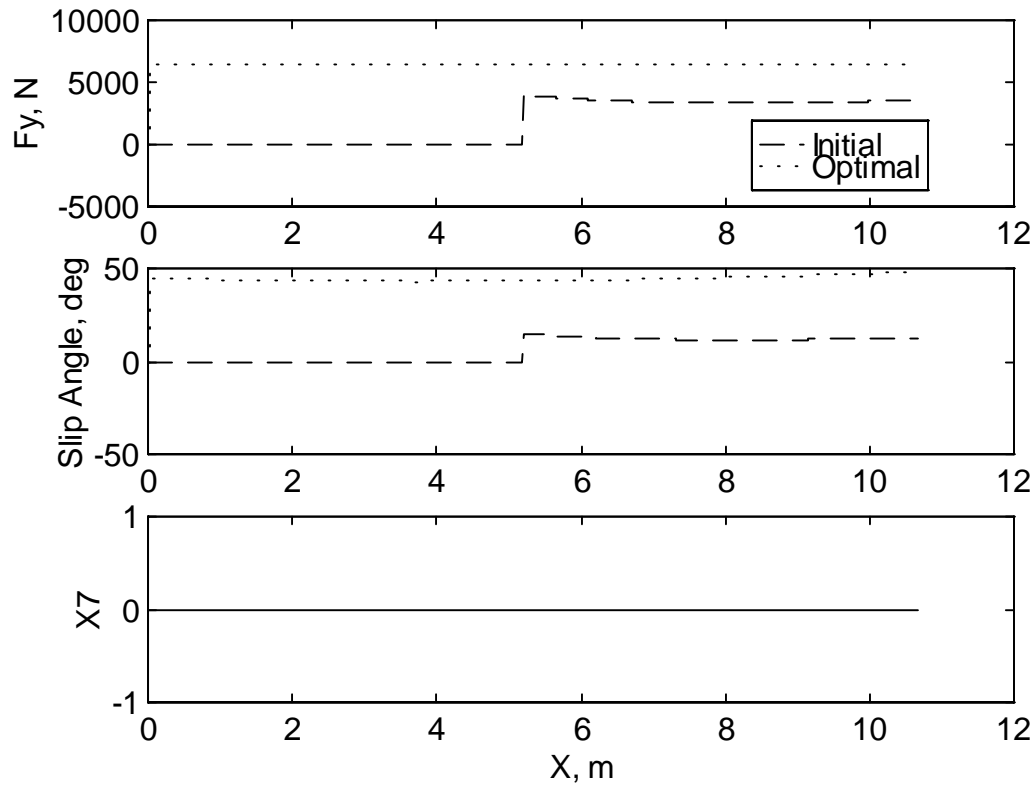


**Figure 4.40 Case No. 6: Lateral Force, Slip Angle, & Vehicle Speed Constraint**

The lateral force is optimized for this particular simulation. The optimal slip angle shows the same trend. The speed constraint variable is zero for the entire path because the maximum speed of 120 mph (27.0 m/s) is not exceeded.

Figure 4.41 shows the path constraint variable, the steering angle constraint variable, and the longitudinal force constraint variable.

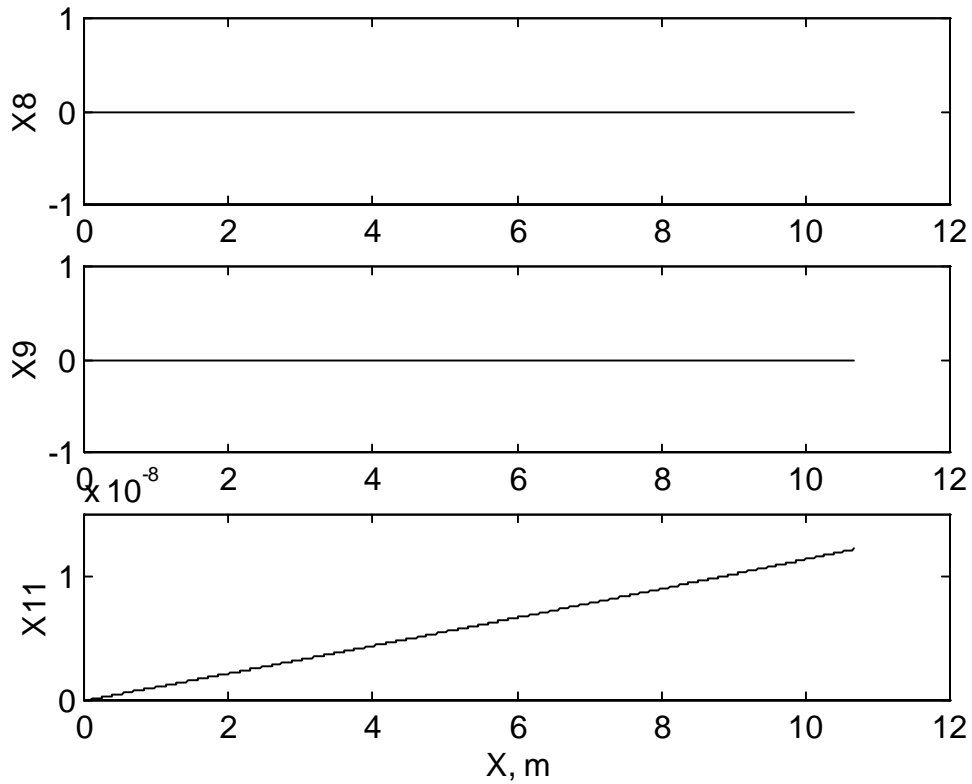


**Figure 4.41 Case No. 6: Path Constraint ( $x_8$ ), Steering Angle Constraint ( $x_9$ ), & Longitudinal Force Constraint ( $x_{11}$ )**

None of these variables exceeded the constraint condition defined in the penalty functions, Eqs (3.8), (3.10), and (3.13).

Figure 4.42 shows the augmented state variable describing the maximizing of tire forces function, described in Eq. (3.15), and the resultant tire force.

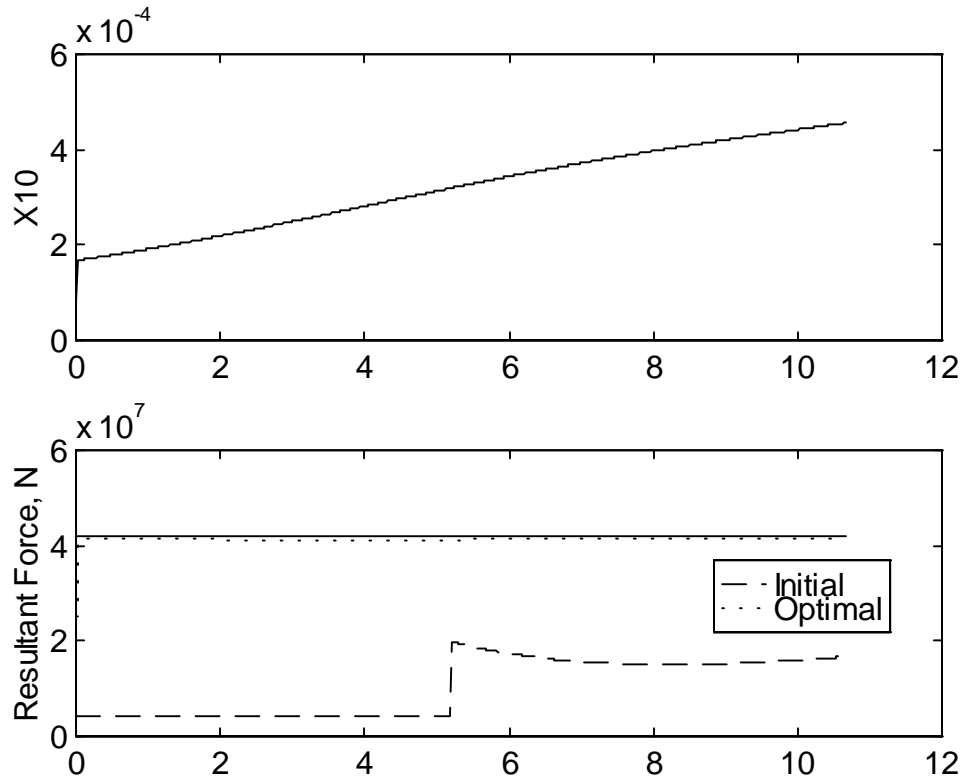


**Figure 4.42 Case No. 6: Maximize Tire Forces Objective Variable, Resultant Force**

$X_{10}$  shows that the front tire force is essentially maximized, its value is almost zero. Therefore it is understandable that the resultant force has such a profile where the optimal resultant force, indicated by the dotted line, lies almost on top of the maximum allowable tire force, corresponding to the friction circle concept, Figure 2.13.



### 4.5.1.3 Case No. 7: Max Tire Force, $V_{\eta} = 20$ m/s, Sine Input

For Case No. 7, the system inputs are a sine wave steering angles, and a constant longitudinal force as shown in Table 4.18 which lists the initial conditions of the state variables.

**Table 4.18 Case No. 7: Initial Values of Vehicle Model**

Variable	Value
$X_1$	0
$X_2$	0
$X_3$	20
$X_4$	0
$X_5$	0
$X_6$	0
$X_7$	0
$X_8$	0
$X_9$	0
$X_{10}$	0
$X_{11}$	0

Figure 4.43 shows the optimized steering angle and longitudinal force, indicated by the dotted line, plotted against the initial condition indicated by the dashed line.

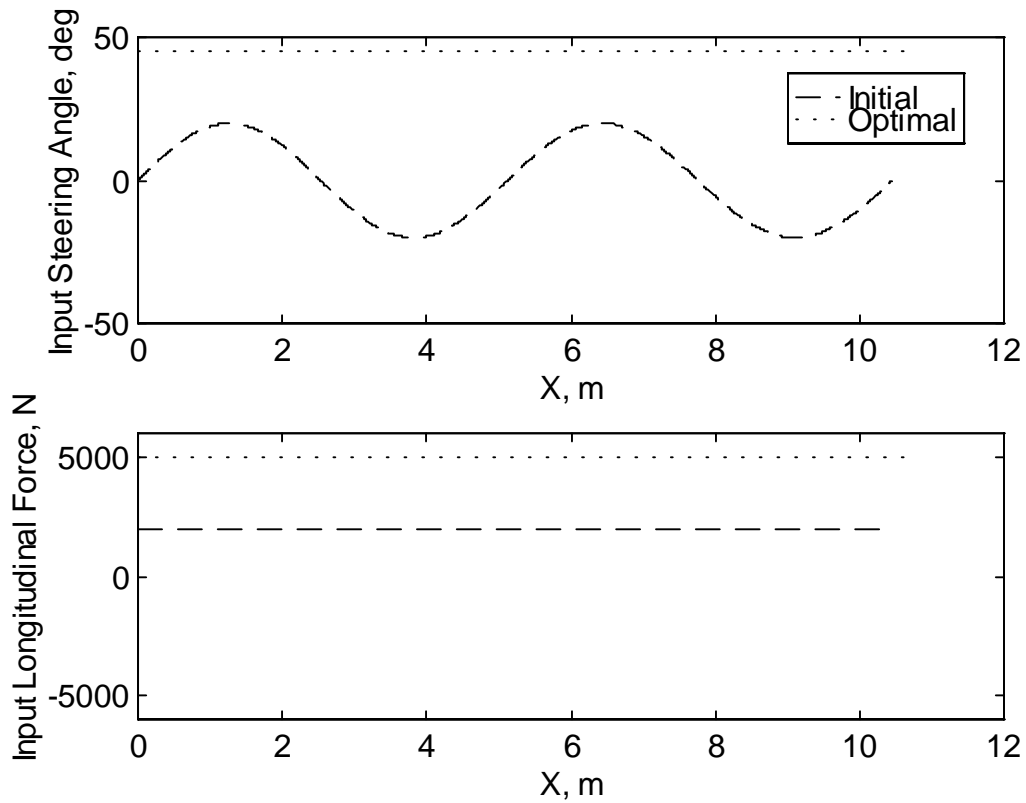


**Figure 4.43 Case No. 7 Optimal System Input**

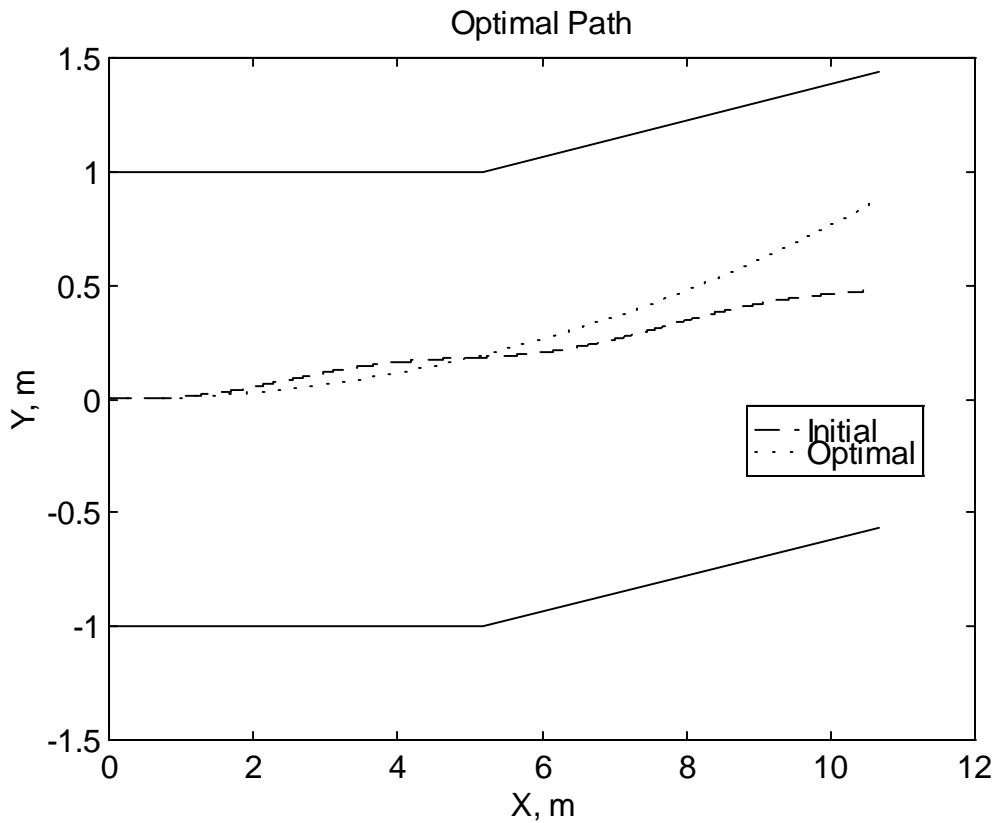
The steering angle is at full lock. In actuality, the optimization routine may have saturated on these values because if the algorithm converges on a larger value than defined in Eq. (3.6), the steering angle becomes saturated. The constants A, B, and C for the sine wave steering function, from Eq. (4.1), seen by the vehicle model are shown in Table 4.19

**Table 4.19 Case No. 7: Optimal Values of the Sine Wave Steering Input**

Variable	Value
A	45
B	45
C	-0.684
t	0.525

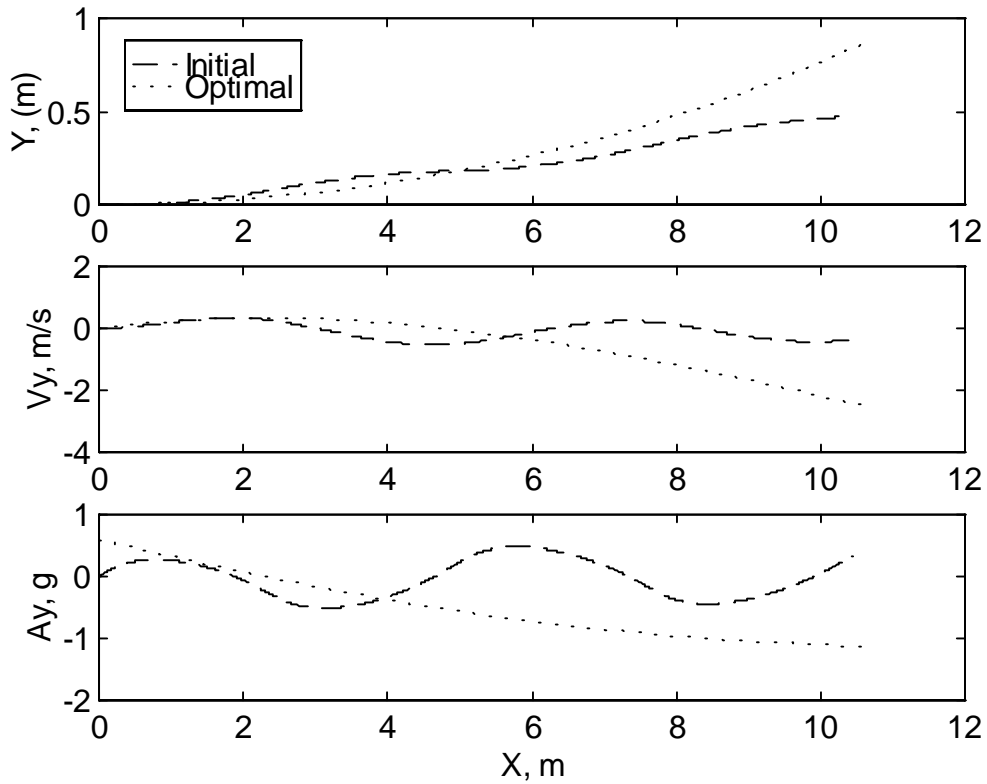
As anticipated, both the steering angle and the longitudinal force are saturated to generate the maximum front tire force.

Figure 4.44 shows the optimal path of the vehicle. The path is a curve generated by full lock steering angle and full throttle longitudinal force.



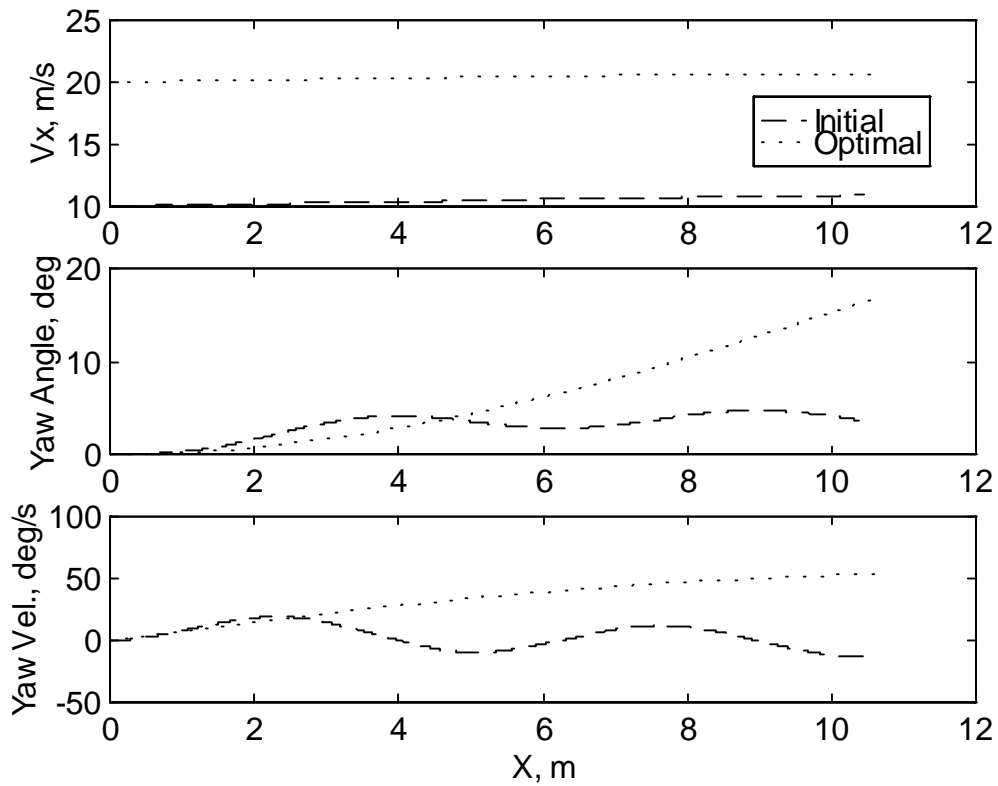
**Figure 4.44 Case No. 7 Optimal Vehicle Path**

Figure 4.45 shows the lateral position, the lateral velocity, and the lateral acceleration of the vehicle at the optimal condition. The lateral position, velocity and acceleration all demonstrate relatively larger lateral amplitudes than the initial condition, resulting in larger front tire forces.



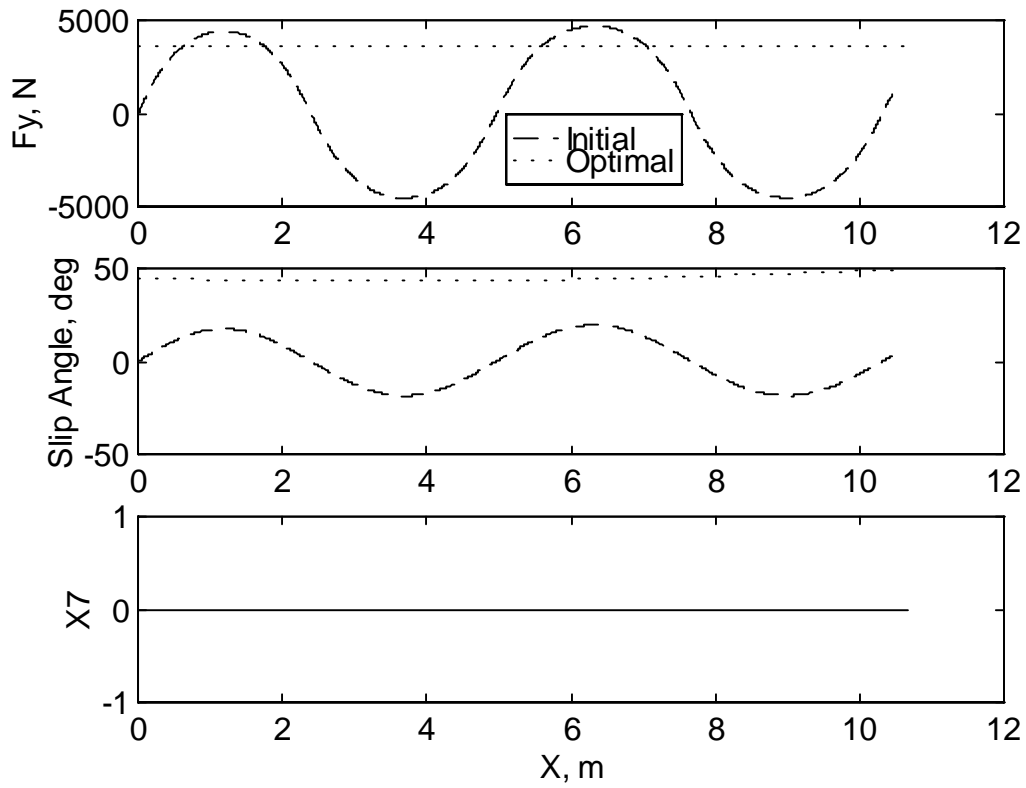
**Figure 4.45 Case No. 7: Lateral Position, Lateral Velocity, & Lateral Acceleration**

Figure 4.46 shows the longitudinal velocity, the yaw angle, and the yaw velocity of the vehicle at the optimal condition. The longitudinal velocity shows a small increase even though there is full throttle longitudinal force. This is because there is large lateral motion caused by the optimal steering angle. As for the optimal yaw angle and velocity, they have larger amplitudes due to the fact that there is larger steering angle input.



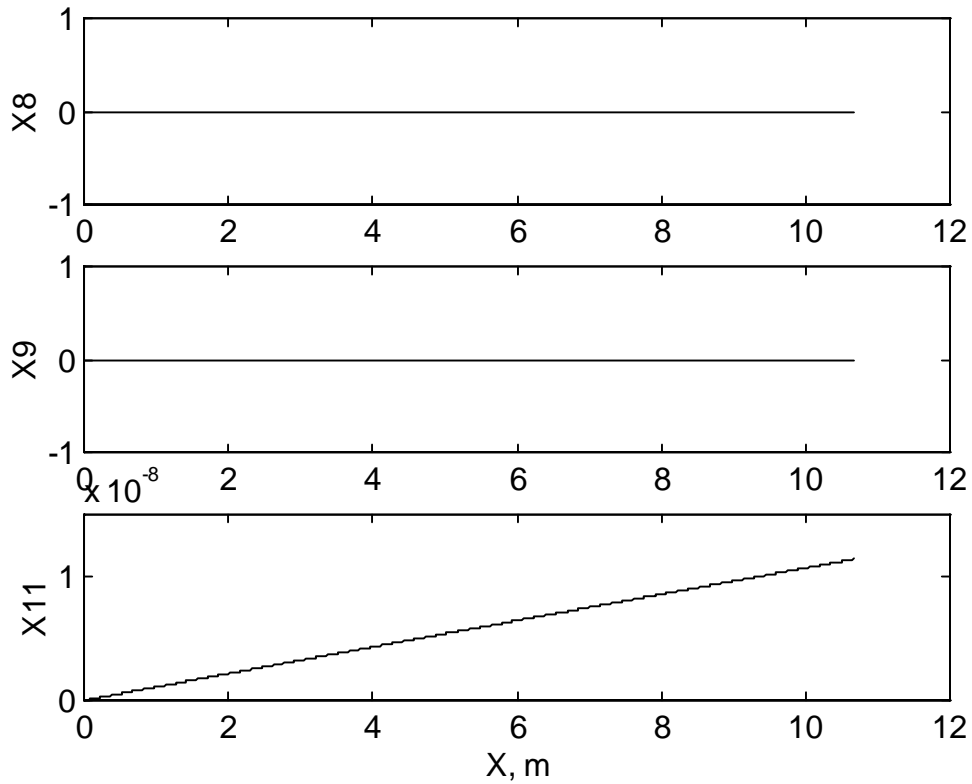
**Figure 4.46 Case No. 7: Longitudinal Velocity, Yaw Angle, & Yaw Velocity**

Figure 4.47 shows the optimal lateral force, the slip angle, and the speed constraint condition. Both the lateral force and the slip angle are relatively high corresponding to large steering angle. The speed constraint variable is zero for the entire path because the maximum speed of 120 mph (27.0 m/s) is not exceeded.



**Figure 4.47 Case No. 7: Lateral Force, Slip Angle, & Vehicle Speed Constraint**

Figure 4.48 shows the path constraint variable, the steering angle constraint variable, and the longitudinal force constraint variable.



**Figure 4.48 Case No. 7: Path Constraint ( $x_8$ ), Steering Angle Constraint ( $x_9$ ), & Longitudinal Force Constraint ( $x_{11}$ )**

None of these variables exceeded the constraint condition defined in the penalty functions, Eqs. (3.8), (3.10), and (3.13).

Figure 4.49 shows the augmented state variable describing the maximizing of tire forces function, described in Eq. (3.15), and the resultant tire force.

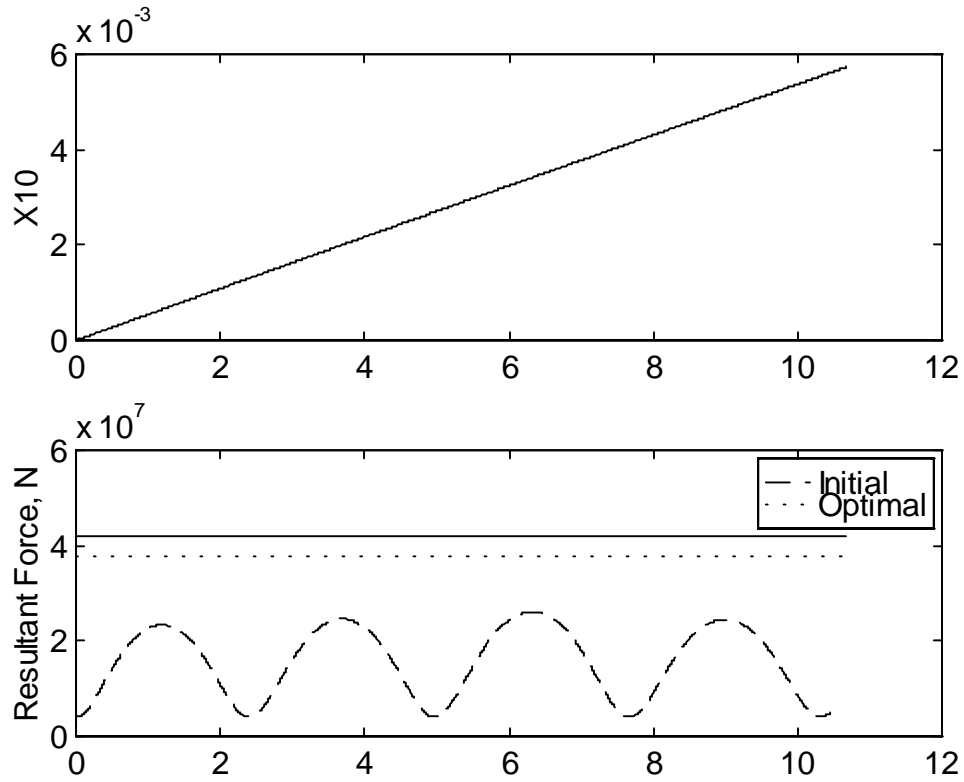


**Figure 4.49 Case No. 7: Maximize Tire Forces Objective Variable, Resultant Force**

$X_{10}$  shows how close the front tire force is to the maximum allowable, therefore it is understandable that the optimal resultant force has such a profile. The optimal resultant force of the tire also shows the effectiveness of the optimization algorithm where the value of the optimal condition is significantly larger than the initial condition.



#### 4.5.2.1 Case No. 8: Max. Tire Forces, $V_{\eta} = 10$ m/s, Step Input

For Case No. 8, the system inputs are a series of step steering angles, and a constant longitudinal force as shown in Table 4.20, which lists the initial conditions of the dynamic variables.

**Table 4.20 Case No. 8: Initial Values of Step/Two-Section Track Simulation**

Variable	Value
$X_1$	0
$X_2$	0
$X_3$	10
$X_4$	0
$X_5$	0
$X_6$	0
$X_7$	0
$X_8$	0
$X_9$	0
$X_{10}$	0
$X_{11}$	0

Figure 4.50. These values were selected so the initial response of the vehicle would be moderated and the vehicle would stay within the boundaries of the track. It also shows the optimized steering angle and longitudinal force. These optimal system inputs best satisfy the objective function that maximizes front tire forces.

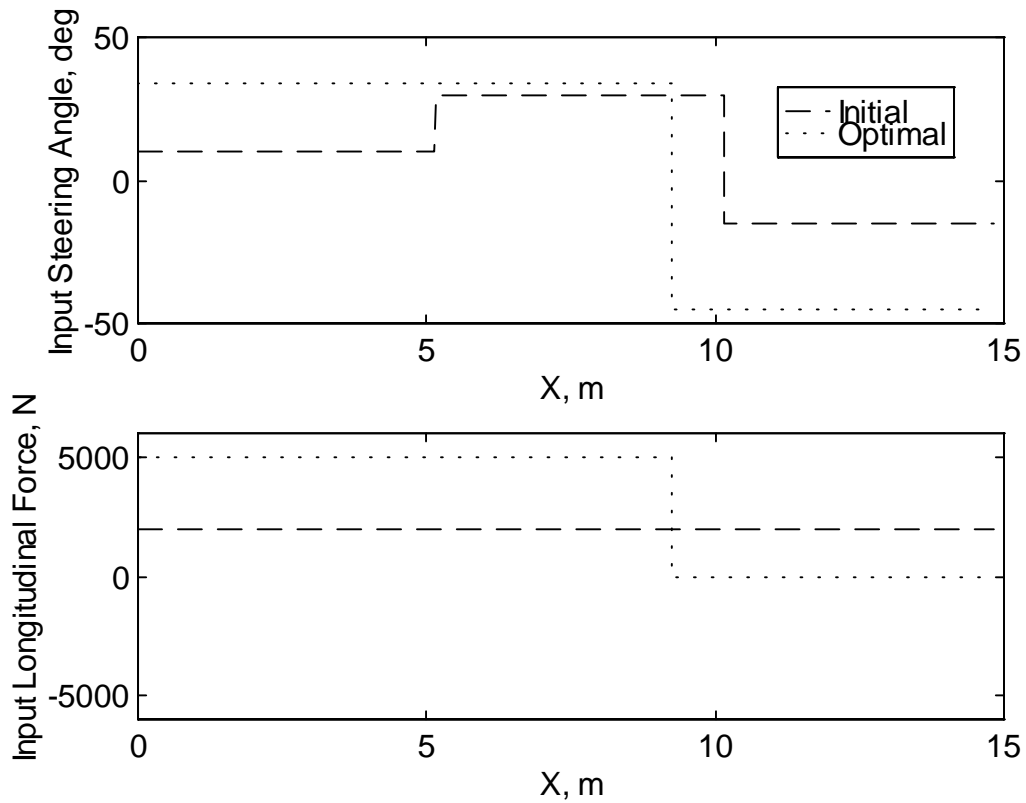


**Figure 4.50 Case No. 8 Optimal System Input**

Table 4.21 lists the values of the optimal system input variables of this case.

**Table 4.21 Values of Optimal System Inputs for Step Input/Three-Section Track**

Track Section	Variable	Value
1	$\delta$	14.899 deg
	$P_f$	2038.21 N
	t	0.001 sec
2	$\delta$	33.578 deg
	$P_f$	5000 N
	t	0.871 sec.
3	$\delta$	-45 deg
	$P_f$	-18.21 N
	t	0.550 sec

where

$\delta$  = steering angle

$P_f$  = longitudinal force

$t$  = time

Figure 4.51 shows the optimal path of the vehicle, indicated by the dotted line, plotted against the initial condition indicated by the dashed line.

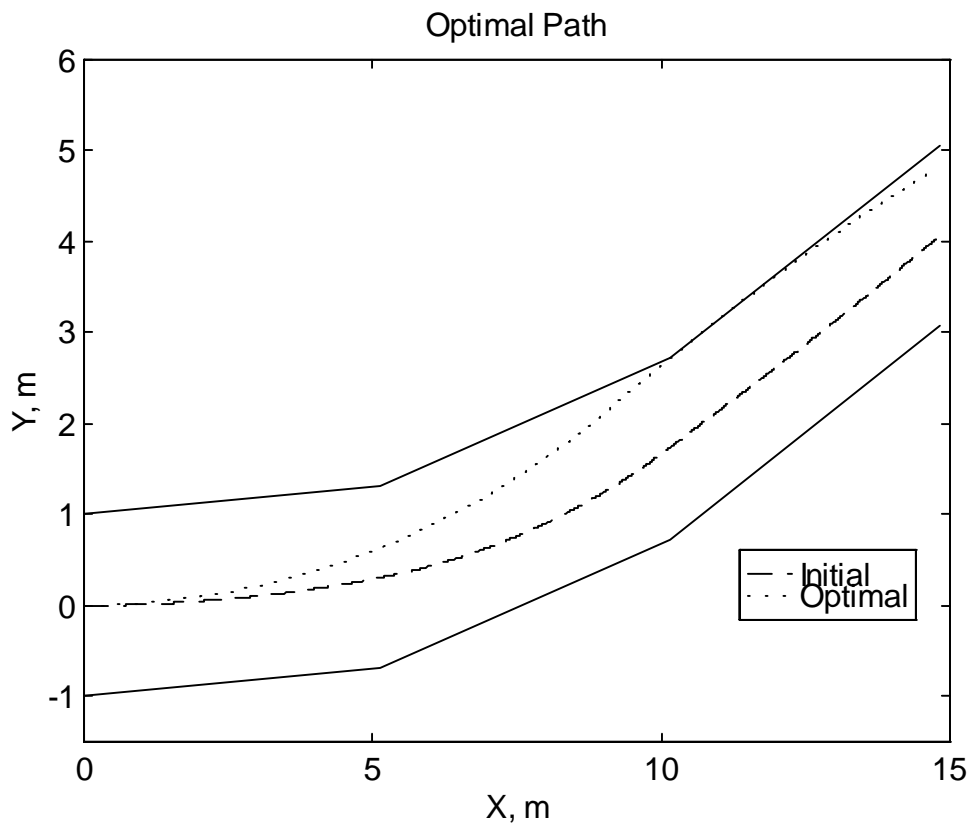


**Figure 4.51 Case No. 8 Optimal Vehicle Path**

The path has more curvature than the initial path. The vehicle almost went outside of the boundary, however the optimization routine restricted it and forced the vehicle back inside.

Figure 4.52 shows the lateral position, the lateral velocity, and the lateral acceleration of the vehicle at the optimal condition.

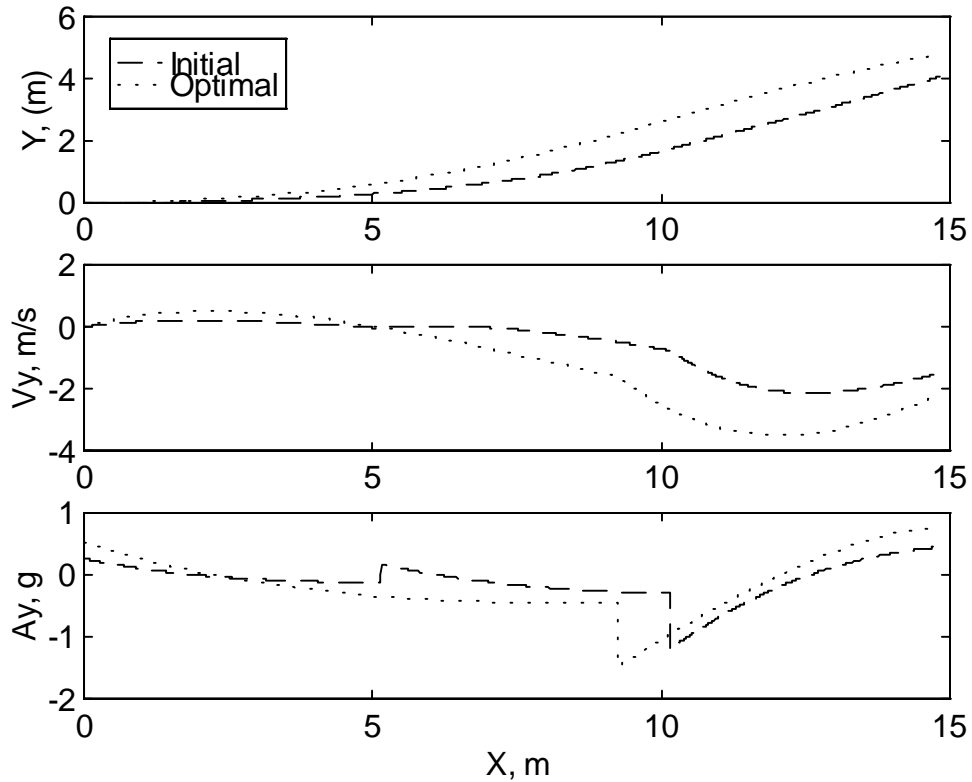


**Figure 4.52 Case No. 8: Lateral Position, Lateral Velocity, & Lateral Acceleration**

These variables consistently have larger amplitudes than the initial ones. This satisfies the fact that the front tire forces are being maximized.

Figure 4.53 shows the longitudinal velocity, the yaw angle, and the yaw velocity of the vehicle at the optimal condition.

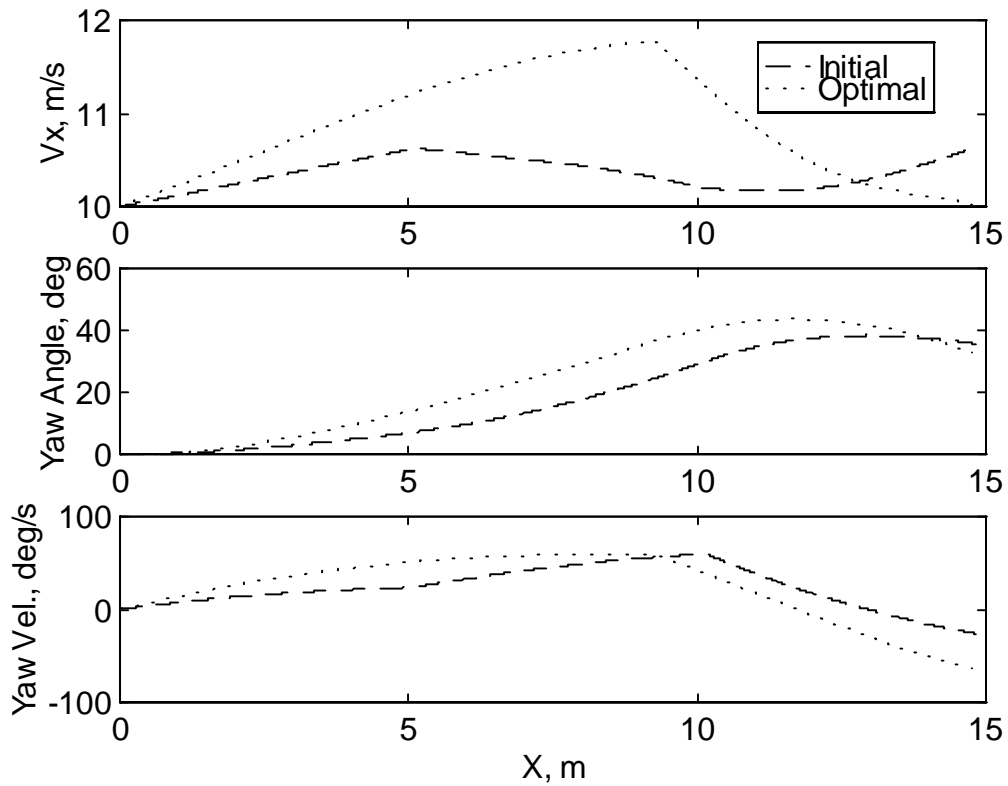


**Figure 4.53 Case No. 8: Longitudinal Velocity, Yaw Angle, & Yaw Velocity**

The longitudinal velocity shows an increase in the beginning of the path and then a sharp decrease. This response corresponds to the longitudinal force input being full throttle at the beginning and then switches over to braking towards the end of the path. The yaw angle and velocity show larger amplitudes and sharper changes corresponding to the shape of the steering angle input.

Figure 4.54 shows the lateral force, the slip angle, and the speed constraint condition.

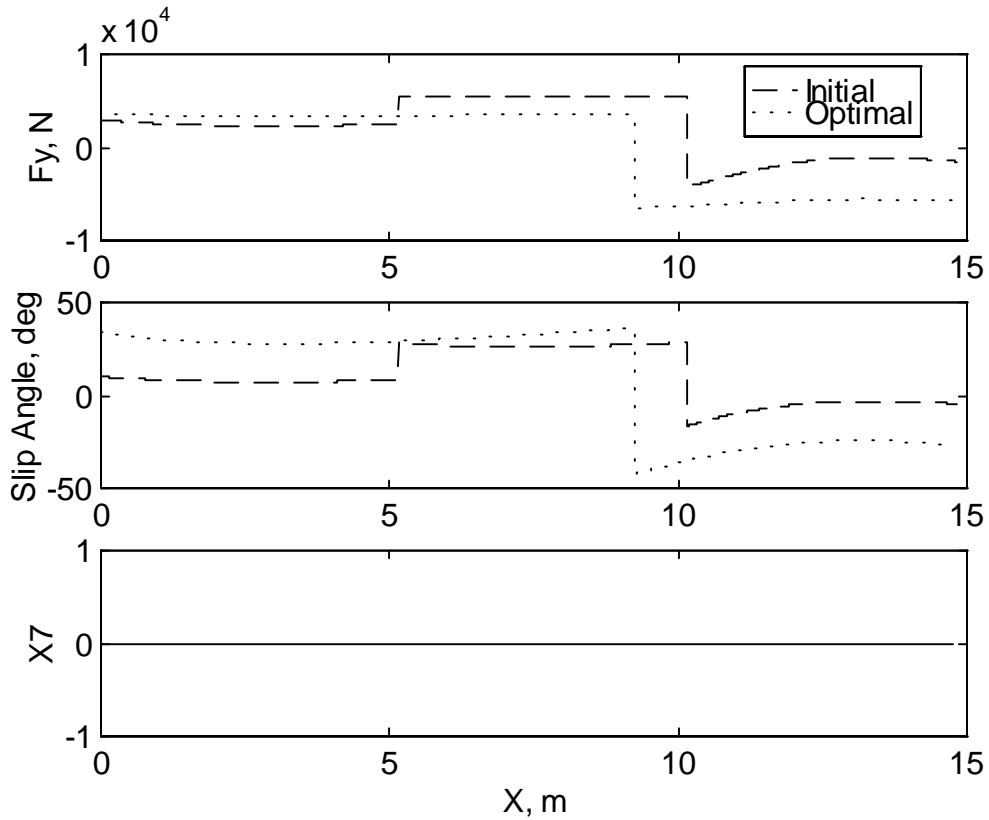


**Figure 4.54 Case No. 8: Lateral Force, Slip Angle, & Vehicle Speed Constraint**

The optimal lateral force is less than the initial one at certain points along the path. The slip angle shows the optimal condition being higher than the initial condition through most parts of the path. This is consistent with the optimal steering angle input. The speed constraint variable is zero for the entire path because the maximum speed of 120 mph (27.0 m/s) is not exceeded.

Figure 4.55 shows the path constraint variable, the steering angle constraint variable, and the longitudinal force constraint variable.

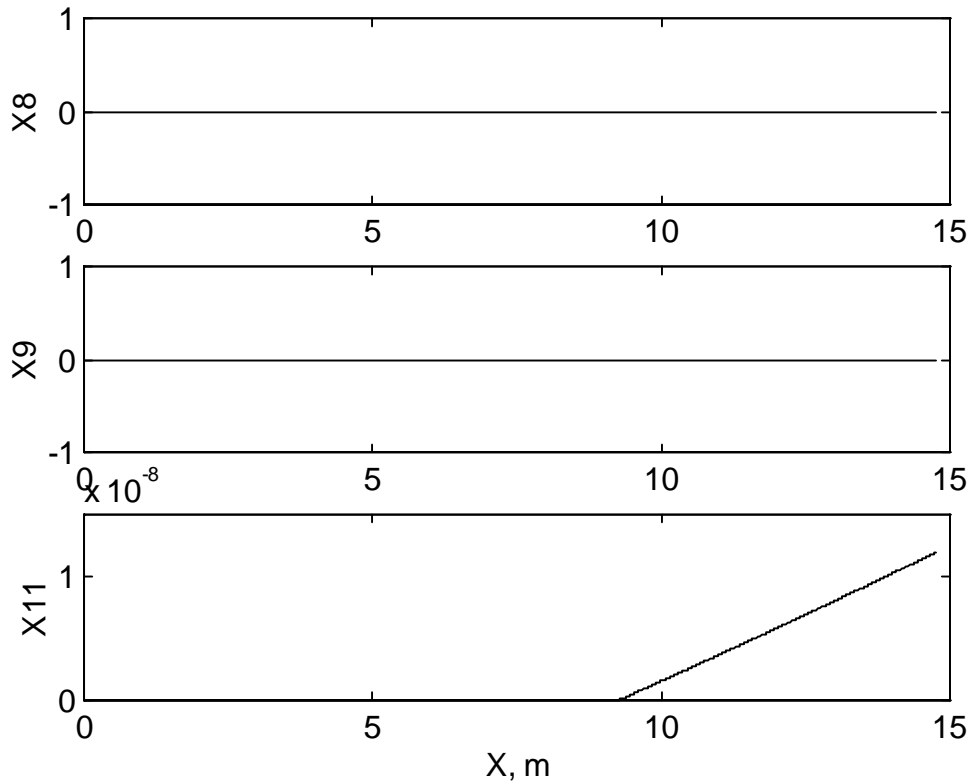


**Figure 4.55 Case No. 8: Path Constraint ( $x_8$ ), Steering Angle Constraint ( $x_9$ ), & Longitudinal Force Constraint ( $x_{11}$ )**

None of these variables exceeded the constraint condition defined in the penalty functions, Eqs. (3.8), (3.10), and (3.13).

Figure 4.56 shows the augmented state variable describing the maximization of tire forces function, described in Eq. (3.15), and the resultant tire force.

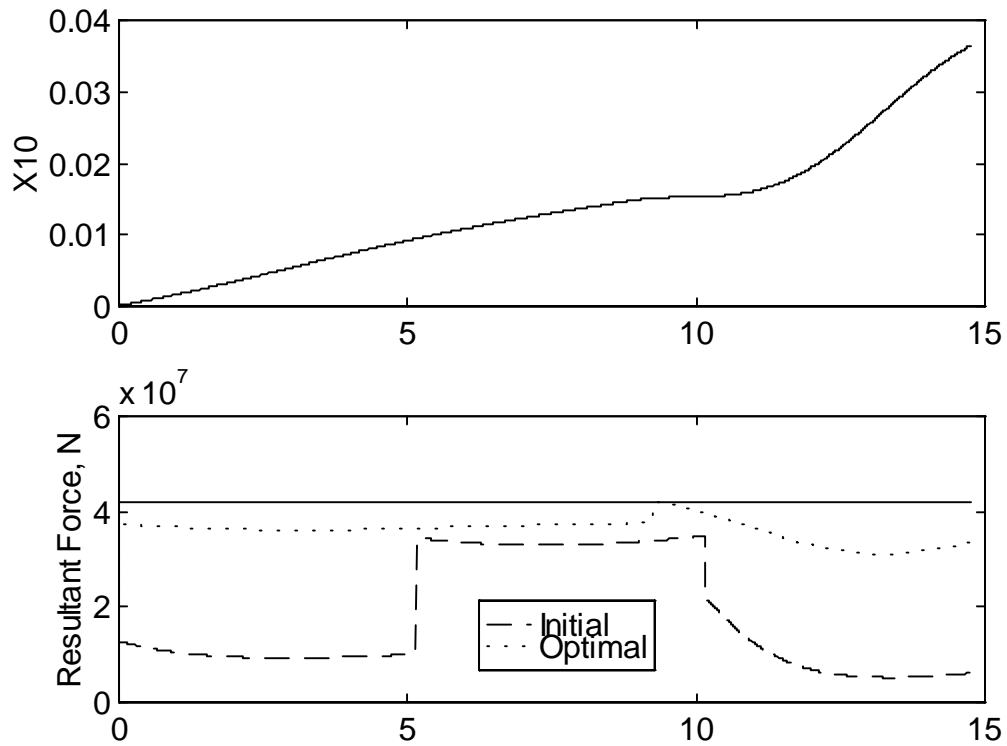


**Figure 4.60 Case No. 8: Maximize Tire Forces Objective Variable, Resultant Force**

$X_{10}$  shows how close the front tire force is to the maximum allowable. Therefore it is understandable that the resultant force has such a profile. Again the optimization routine is effective in attempting to maximize the resultant tire forces, where the optimal resultant force is larger than the initial condition.